Electromagnetic semitransparent δ-function plate: Casimir interaction energy between parallel infinitesimally thin plates

Prachi Parashar, Kimball A. Milton, K. V. Shajesh, and M. Schaden

Electromagnetic semitransparent δ-function plate: Casimir interaction energy between parallel infinitesimally thin plates

Prachi Parashar* and Kimball A. Milton†

Homer L. Dodge Department of Physics and Astronomy,
University of Oklahoma, Norman, OK 73019, USA

K. V. Shajesh^c§ and M. Schaden¶

Department of Physics, Rutgers, The State University of New Jersey, Newark, NJ 07102, USA

We derive boundary conditions for electromagnetic fields on a δ-function plate. The optical properties of such a plate are shown to necessarily be anisotropic in that they only depend on the transverse properties of the plate. We unambiguously obtain the boundary conditions for a perfectly conducting δ-function plate in the limit of infinite dielectric response. We show that a material does not "optically vanish" in the thin-plate limit. The thin-plate limit of a plasma slab of thickness d with plasma frequency $\omega_p^2 = \zeta_p/d$ reduces to a δ-function plate for frequencies $(\omega = i\zeta)$ satisfying $\zeta d \ll \sqrt{\zeta_p d} \ll 1$. We show that the Casimir interaction energy between two parallel perfectly conducting δ-function plates is the same as that for parallel perfectly conducting slabs. Similarly, we show that the interaction energy between an atom and a perfect electrically conducting δ-function plate is the usual Casimir-Polder energy, which is verified by considering the thin-plate limit of dielectric slabs. The "thick" and "thin" boundary conditions considered by Bordag are found to be identical in the sense that they lead to the same electromagnetic fields.

PACS numbers: 11.80.La, 12.20.-m, 41.20.Cv, 77.55.-g

I. INTRODUCTION

Idealized infinitesimally thin perfectly conducting surfaces are often envisaged to decouple electromagnetically two regions in space. Boyer in 1968 [1] found that the Casimir energy of such a thin perfectly conducting spherical shell contributes a radial outward pressure on the surface of the shell. The repulsive nature of this force, unlike the attractive Casimir force between parallel perfectly conducting plates [2], has remained poorly understood, but general systematics are becoming clearer [3–5]. To investigate the physical nature of Boyer's result, Barton in Ref. [6–8] used a hydrodynamic model developed in Refs. [9, 10] to study the Casimir energy of a spherical plasma shell as a continuum model of interactions in C_{60} and C_{70} molecules. Barton observed that an infinitesimally thin conducting surface imposes non-trivial boundary conditions on the electromagnetic fields and in Refs. [11, 12] considered "a fluid model of an infinitesimally thin plasma sheet to describe a single base plane from graphite," in which boundary conditions on such a plate are derived by integrating across the plate. These boundary conditions are broadly referred to as the plasma shell model.

A δ-function as a model for an infinitesimally thin conducting surface was first used in Refs. [13, 14]. Reference [15] proposed that perfect electrical conductors could satisfy two independent boundary conditions, dubbed "thick" and "thin" boundary conditions in Ref. [16]. Bordag in Ref. [17] reported that the Casimir-Polder force calculated with "thin" boundary conditions is 13% lower than that obtained with "thick" boundary conditions. Variations of this calculation has been presented again in Refs. [16] and [18]. This has led to confusion in the understanding of the boundary conditions on a δ-function plate, which eventually has also entered into discussions on graphene. We resolve the issue by showing that all the three boundary conditions: Barton's plasma shell model, and Bordag's "thick" and "thin" boundary conditions, are identical.

In this paper we consider an idealized infinitesimally thin material whose electric and magnetic properties are described by an electric permittivity and a magnetic permeability written in terms of a δ-function,

$$\boldsymbol{\varepsilon}(z) - \mathbf{1} = \boldsymbol{\lambda}_e \delta(z), \tag{1a}$$

$$\boldsymbol{\mu}(z) - \mathbf{1} = \boldsymbol{\lambda}_g \delta(z). \tag{1b}$$

^c Present address: Department of Energy and Process Engineering, Norwegian University of Science and Technology, N-7491 Trondheim, Norway
* prachi@nhn.ou.edu
† milton@nhn.ou.edu; http://www.nhn.ou.edu/~milton
§ shajesh@andromeda.rutgers.edu; http://www.nhn.ou.edu/~shajesh
¶ mschaden@andromeda.rutgers.edu; http://andromeda.rutgers.edu/~physics/mschaden.htm

Following Refs. [19, 20] we call this a semitransparent δ-function plate. $\boldsymbol{\lambda}_e$ and $\boldsymbol{\lambda}_g$ in this model have dimensions of length, and are in general frequency dependent. The δ-function in Eq. (1) should be thought of as a limit of a sequence of functions that are symmetric about the plane $z = 0$ [21]. The electric permittivity and magnetic permeability is assumed isotropic in the plane of the plate only. The distinction of parallel and perpendicular components will be made in reference to the z-direction chosen normal to the plane of the plate, for example, $\mathbf{k}_\perp$ will represent components of $\mathbf{k}$ perpendicular to the normal. The tensor structure of $\boldsymbol{\lambda}_e$ and $\boldsymbol{\lambda}_g$ is chosen to be diagonal in the xyz-coordinate system for simplicity.

In Sec. II we study Maxwell's equations in the presence of δ-function plates described by Eqs. (1). Employing a Gaussian surface integral and an Amperian loop integral across the plate we find additional non-vanishing contributions in the boundary conditions due to the δ-functions in Eqs. (1). They imply anisotropic optical properties for a semitransparent δ-function plate. These boundary conditions are derived for the case of a δ-function plate sandwiched between two uniaxial materials and reduce to the conventional boundary conditions when $\boldsymbol{\lambda}_e = 0$ and $\boldsymbol{\lambda}_g = 0$, and are consistent with those derived by Barton in Ref. [11] for a purely electric δ-function plate. The anisotropy in Barton's plasma sheet model arises implicitly due to the requirement that any displacements in the plasma are tangential to the plate.

In Sec. II B magnetic and electric Green's functions, representing the two independent modes, are constructed and the fields are defined in terms of the Green's dyadics. In Sec. III the boundary conditions derived for the fields are transcribed onto the magnetic and electric Green's functions. We unambiguously derive solutions for these Green's functions, which determine the reflection and transmission coefficients for a semitransparent δ-function plate. Our solutions generalize Barton's by allowing for non-trivial magnetic properties of a δ-function plate. The rate of change of energy density of the electromagnetic field is shown to be balanced by the energy flux across the plate. This statement of the conservation of energy is expressed in terms of reflection and transmission coefficients of a δ-function plate. Both a perfect electrically conducting δ-function plate with vanishing magnetic susceptibility, and a perfect magnetically conducting δ-function plate with vanishing electric response, are perfect reflectors that do not transmit energy across the plate. By contrast, a perfect electrically and magnetically conducting δ-function plate is a perfect transmitter of energy while introducing a phase shift of $180°$ in the transmitted fields, and would pass the test for invisibility. A split coherent laser beam incident on such a plate from both sides would extinguish itself.

In Sec. III B we derive boundary conditions across a perfect electrically conducting δ-function plate by taking the limit of infinite dielectric response. We find that even though the tangential component of the electric field vanishes on a δ-function plate, the corresponding component of electric displacement field does not, unambiguously specifying the discontinuity in the normal component of the electric displacement field across the δ-function plate. We clarify how a semi-infinite isotropic dielectric slab and an (anisotropic) δ-function plate lead to the same boundary conditions and the same physics in the limit of perfect conduction.

Following Ref. [22], we investigate the feasibility of physically realizing a semitransparent δ-function plate in Sec. IV. In contrast to naive expectations we show that a material does not necessarily optically vanish in the limit of zero thickness. The thin-plate limit, in which the optical properties of a dielectric slab of thickness d with plasma frequency $\omega_p^2 = \zeta_p/d$ may be approximated by a δ-function plate, is shown to be satisfied for frequencies in the range $\zeta d \ll \sqrt{\zeta_p d} \ll 1$. By modelling the charge carriers in a conducting slab as a Fermi gas with Neumann boundary conditions we explore the conditions necessary for the realization of a two-dimensional conducting sheet. In this model we relate the optical properties of a δ-function plate with the plasma frequency of the two-dimensional plasma.

In Sec. V the interaction energy between two parallel δ-function plates is obtained from their optical properties. We explicitly show that the interaction energy between parallel perfect electrically conducting δ-function plates is the Casimir energy between two ideal metallic slabs. We further verify that the interaction energy between parallel anisotropic slabs in the limit of vanishing thickness (thin-plate limit) also reproduces the interaction energy for parallel δ-function plates. In Sec. VI the interaction energy between an atom and a semitransparent δ-function plate is calculated. In the perfect conductor limit this interaction energy is just the usual Casimir-Polder energy between an atom and an ideal metallic slab. This is verified independently using the thin-plate limit. We show that all of the three boundary conditions discussed in the literature to understand the electrodynamics of a δ-function plate—Barton's plasma shell model and Bordag's "thick" and "thin" boundary conditions—are physically identical. In the final section we conclude by discussing our results.

In Appendix A we show that a function with a step discontinuity when evaluated at the point of discontinuity should be interpreted as the average of the function's left and right limiting values. In Appendices B and C the details of the calculations leading to the Casimir interaction energy between two semitransparent δ-function plates and two anisotropic slabs are presented.

II. INFINITESIMALLY THIN δ-FUNCTION PLATES

We consider a semitransparent δ-function plate described by Eqs. (1) and restrict our analysis to uniaxial materials with the optical axis oriented normal to the plane of the plate, chosen as the $\hat{\mathbf{z}}$ direction of a Cartesian coordinate system. We thus consider materials whose optical properties are represented by

$$\boldsymbol{\lambda}_e = \lambda_e^\perp \, \mathbf{1}_\perp + \lambda_e^{||} \, \hat{\mathbf{z}} \, \hat{\mathbf{z}}, \tag{2a}$$

$$\boldsymbol{\lambda}_g = \lambda_g^\perp \, \mathbf{1}_\perp + \lambda_g^{||} \, \hat{\mathbf{z}} \, \hat{\mathbf{z}}, \tag{2b}$$

where $\lambda_{e,g}^\perp$ and $\lambda_{e,g}^{||}$, in general are frequency dependent. In Heaviside-Lorentz units the monochromatic components proportional to $\exp(-i\omega t)$ of Maxwell's equations in the absence of charges and currents are

$$\boldsymbol{\nabla} \times \mathbf{E} = i\omega \mathbf{B}, \tag{3a}$$

$$-\boldsymbol{\nabla} \times \mathbf{H} = i\omega(\mathbf{D} + \mathbf{P}), \tag{3b}$$

which implies $\boldsymbol{\nabla} \cdot \mathbf{B} = 0$, and $\boldsymbol{\nabla} \cdot (\mathbf{D} + \mathbf{P}) = 0$, where $\mathbf{P}$ is an external source of polarization. We in the following neglect non-linear responses and assume that the fields $\mathbf{D}$ and $\mathbf{B}$ are linearly dependent on the electric and magnetic fields $\mathbf{E}$ and $\mathbf{H}$ as

$$\mathbf{D}(\mathbf{x}, \omega) = \boldsymbol{\varepsilon}(\mathbf{x}; \omega) \cdot \mathbf{E}(\mathbf{x}, \omega), \tag{4a}$$

$$\mathbf{B}(\mathbf{x}, \omega) = \boldsymbol{\mu}(\mathbf{x}; \omega) \cdot \mathbf{H}(\mathbf{x}, \omega). \tag{4b}$$

Exploiting translational symmetry in the plane of the plate and rotational symmetry about the normal $\hat{\mathbf{z}}$ direction, we may consider a plane wave with wave-numbers k_x and k_y and choose $k_y = 0$ without loss of generality. We thus can write $\boldsymbol{\nabla} = ik_\perp \hat{\mathbf{x}} + \hat{\mathbf{z}} \partial_z$, with $k_\perp = k_x$. Maxwell's equations in Eqs. (3) thus decouple into those for two modes[1]: the transverse magnetic mode (TM or E-mode) involves the field components (E_1, H_2, E_3):

$$H_2(z) = -\frac{\omega}{k_\perp} D_3(z) - \frac{\omega}{k_\perp} P_3(z), \tag{5a}$$

$$\frac{\partial}{\partial z} D_3(z) = -ik_\perp D_1(z) - ik_\perp P_1(z) - \frac{\partial}{\partial z} P_3(z), \tag{5b}$$

$$\frac{\partial}{\partial z} E_1(z) = ik_\perp E_3(z) + i\omega B_2(z), \tag{5c}$$

and the transverse electric mode (TE or H-mode) involves the field components (H_1, E_2, H_3):

$$E_2(z) = \frac{\omega}{k_\perp} B_3(z), \tag{6a}$$

$$\frac{\partial}{\partial z} B_3(z) = -ik_\perp B_1(z), \tag{6b}$$

$$\frac{\partial}{\partial z} H_1(z) = ik_\perp H_3(z) - i\omega D_2(z) - i\omega P_2(z). \tag{6c}$$

The Maxwell's equations in Eqs. (5) and (6), which are in first order form, can be combined to yield the second order differential equations [with $\boldsymbol{\varepsilon} = \mathrm{diag}(\varepsilon^\perp, \varepsilon^\perp, \varepsilon^{||})$ and $\boldsymbol{\mu} = \mathrm{diag}(\mu^\perp, \mu^\perp, \mu^{||})$]

$$\left[-\frac{\partial}{\partial z} \frac{1}{\varepsilon^\perp(z)} \frac{\partial}{\partial z} + \frac{k_\perp^2}{\varepsilon^{||}(z)} - \omega^2 \mu^\perp(z) \right] H_2(z) = -i\omega \frac{\partial}{\partial z} \frac{P_1(z)}{\varepsilon^\perp(z)} - \omega k_\perp \frac{P_3(z)}{\varepsilon^{||}(z)}, \tag{7a}$$

$$\left[-\frac{\partial}{\partial z} \frac{1}{\mu^\perp(z)} \frac{\partial}{\partial z} + \frac{k_\perp^2}{\mu^{||}(z)} - \omega^2 \varepsilon^\perp(z) \right] E_2(z) = \omega^2 P_2(z). \tag{7b}$$

The remaining field components can be expressed in terms of $H_2(z)$ and $E_2(z)$: $E_1(z)$ using Eqs. (5a) and (5b), $E_3(z)$ using Eq. (5a), $H_1(z)$ using Eqs. (6a) and (6b), and $H_3(z)$ using Eq. (6a).

---

[1] In the context of wave-guides these modes refer to the direction of propagation ($\hat{\mathbf{x}}$ in our case). TM (TE) modes have no magnetic (electric) field in the direction of propagation, whereas E(H)-modes have a electric (magnetic) field component in the direction of propagation. Note that the same can be thought of relative to the direction normal to the plane ($\hat{\mathbf{z}}$).

A. Boundary conditions

Boundary conditions for electromagnetic fields due to the presence of a single semitransparent δ-function plate in vacuum, or such a plate sandwiched between two adjacent semi-infinite slabs, are derived by integrating Maxwell's equations in Eqs. (3), or more explicitly Eqs. (5) and (6), across the δ-function plate positioned at $z = a$. We require electric and magnetic fields to be free of δ-function type singularities,

$$\lim_{\delta \to 0} \int_{a-\delta}^{a+\delta} dz\, \mathbf{E}(z) = 0, \qquad \text{and} \qquad \lim_{\delta \to 0} \int_{a-\delta}^{a+\delta} dz\, \mathbf{H}(z) = 0, \tag{8}$$

implying that the δ-function singularities of $\boldsymbol{\varepsilon}$ and $\boldsymbol{\mu}$ in Eqs. (1) are completely contained in $\mathbf{D}$ and $\mathbf{B}$ as a consequence of Eqs. (4). To illustrate this explicitly let us for the moment consider the case of $\boldsymbol{\lambda}_g = \mathbf{0}$ and $\lambda_e^{||} = 0$. Then, for any given source distribution $\mathbf{P}$, Eqs. (5) can be combined to yield

$$\left[-\frac{\partial^2}{\partial z^2} + (k_\perp^2 - \omega^2) + (k_\perp^2 - \omega^2)\lambda_e^\perp \delta(z-a) \right] E_1(z) = (k_\perp^2 - \omega^2)P_1(z) - ik_\perp \frac{\partial}{\partial z} P_3(z), \quad \text{for} \quad \boldsymbol{\lambda}_g = \mathbf{0}, \quad \lambda_e^{||} = 0. \tag{9}$$

If $E_1(z)$ were to have a δ-function singularity on the plate, then the derivatives of $E_1(z)$ would have higher order singularities and Eq. (9) can not be consistently balanced. Thus, the conditions in Eq. (8) are necessary for consistency.

The boundary conditions[2] on the TM mode are found, by integrating Eqs. (5), to be

$$\lambda_e^{||} E_3(a) = 0, \tag{10a}$$
$$D_3(a+\delta) - D_3(a-\delta) = -ik_\perp \lambda_e^\perp E_1(a), \tag{10b}$$
$$E_1(a+\delta) - E_1(a-\delta) = i\omega \lambda_g^\perp H_2(a), \tag{10c}$$

and the corresponding boundary conditions on the TE mode are found, by integrating Eqs. (6), to be

$$\lambda_g^{||} H_3(a) = 0, \tag{11a}$$
$$B_3(a+\delta) - B_3(a-\delta) = -ik_\perp \lambda_g^\perp H_1(a), \tag{11b}$$
$$H_1(a+\delta) - H_1(a-\delta) = -i\omega \lambda_e^\perp E_2(a). \tag{11c}$$

Equations (10) and (11) reduce to the correct boundary conditions at the interface of two semi-infinite slabs without surface charges and currents when the δ-function plate is absent (obtained by omitting terms involving $\lambda_{e,g}^{\perp,||}$'s). Because the position of the polarization source in Eqs. (3) is at our disposal we can choose it to lie outside the integration region to derive Eqs. (10) and (11). In Eqs. (10) and (11) some fields have to be evaluated on the semitransparent δ-function plate, and we will see that $E_3(z)$ and $H_3(z)$ in general are discontinuous at $z = a$. The evaluation of such discontinuous fields at $z = a$ is mathematically ill-defined. But, when the δ-functions in Eq. (1) are interpreted as a limit of a sequence of functions that are symmetric about $z = a$ [21] these fields are readily evaluated as the average of their left and right limits at $z = a$ even if these limits do not coincide (as long as both limits exist). This "averaging prescription" has been proved in Appendix A. The evaluations in Eqs. (10a) and (11a) thus should be understood as averages of the values of the discontinuous function on either side of the semitransparent δ-function plate. This averaging prescription was previously argued on heuristic grounds [24] and was successfully employed to calculate the lateral Casimir force and Casimir torque between semitransparent δ-function surfaces with sinusoidal corrugations for planar as well as cylindrical geometries in Refs. [24] and [25] involving interactions mediated by a scalar field.

Boundary conditions on a semitransparent δ-function plate in Eqs. (10) and (11) were also derived by Barton in Ref. [11]. Barton does not explicitly write Eqs. (10a) and (11a) in Ref. [11] but these conditions are implicit in his model. Equations (10a) and (11a) imply that $\lambda_e^{||} = 0$ unless $E_3(a) = 0$, and $\lambda_g^{||} = 0$ unless $H_3(a) = 0$. One thus can conclude that a semitransparent δ-function plate necessarily is anisotropic in its optical properties. We postpone discussion of the boundary conditions on a perfect electrically conducting δ-function plate until Sec. III B.

---

[2] These boundary conditions differ from those considered in Ref. [23] which attempts to model a δ-function plate in the context of relativistic macroscopic electrodynamics. The boundary conditions we consider here more closely model a δ-function plate with nonrelativistic matter inside. There is no distinction between $\boldsymbol{\lambda}_e$ and $\boldsymbol{\lambda}_g$ in Ref. [23], and although the same Casimir energy is recovered in the perfect conductor limit, their results in general do not agree with those obtained in the present article.

B. Fields and Green's functions

To keep our discussions open to the implications of Eqs. (10a) and (11a) we shall not use isotropic considerations for simplification. We define the magnetic Green's function $g^H(z, z')$, and the electric Green's function $g^E(z, z')$, as the inverse of the differential operators in Eqs. (7), to construct

$$\left[-\frac{\partial}{\partial z} \frac{1}{\varepsilon^\perp(z)} \frac{\partial}{\partial z} + \frac{k_\perp^2}{\varepsilon^{||}(z)} - \omega^2 \mu^\perp(z) \right] g^H(z, z') = \delta(z - z'), \tag{12a}$$

$$\left[-\frac{\partial}{\partial z} \frac{1}{\mu^\perp(z)} \frac{\partial}{\partial z} + \frac{k_\perp^2}{\mu^{||}(z)} - \omega^2 \varepsilon^\perp(z) \right] g^E(z, z') = \delta(z - z'), \tag{12b}$$

written in terms of anisotropic material properties (with isotropy in the plane). The components of the fields are obtained in terms of the Green's functions by inverting Eqs. (7) and the corresponding equations for other components. These are expressed in the form

$$\mathbf{E}(z) = \int dz' \, \boldsymbol{\gamma}(z, z') \cdot \mathbf{P}(z'), \tag{13a}$$

$$\mathbf{H}(z) = \int dz' \, \boldsymbol{\phi}(z, z') \cdot \mathbf{P}(z'), \tag{13b}$$

in terms of the reduced Green's dyadics

$$\boldsymbol{\gamma}(z, z') = \begin{bmatrix} \frac{1}{\varepsilon^\perp(z)} \frac{\partial}{\partial z} \frac{1}{\varepsilon^\perp(z')} \frac{\partial}{\partial z'} g^H(z, z') & 0 & \frac{1}{\varepsilon^\perp(z)} \frac{\partial}{\partial z} \frac{ik_\perp}{\varepsilon^{||}(z')} g^H(z, z') \\ 0 & \omega^2 g^E(z, z') & 0 \\ -\frac{ik_\perp}{\varepsilon^{||}(z)} \frac{1}{\varepsilon^\perp(z')} \frac{\partial}{\partial z'} g^H(z, z') & 0 & -\frac{ik_\perp}{\varepsilon^{||}(z)} \frac{ik_\perp}{\varepsilon^{||}(z')} g^H(z, z') \end{bmatrix} - \delta(z - z') \begin{bmatrix} \frac{1}{\varepsilon^\perp(z)} & 0 & 0 \\ 0 & 0 & 0 \\ 0 & 0 & \frac{1}{\varepsilon^{||}(z)} \end{bmatrix} \tag{14}$$

and

$$\boldsymbol{\phi}(z, z') = i\omega \begin{bmatrix} 0 & \frac{1}{\mu^\perp(z)} \frac{\partial}{\partial z} g^E(z, z') & 0 \\ \frac{1}{\varepsilon^\perp(z')} \frac{\partial}{\partial z'} g^H(z, z') & 0 & \frac{ik_\perp}{\varepsilon^{||}(z')} g^H(z, z') \\ 0 & -\frac{ik_\perp}{\mu^{||}(z)} g^E(z, z') & 0 \end{bmatrix}. \tag{15}$$

These are straightforward generalizations of the Green's dyadics in Ref. [26] to the anisotropic case. Since we have already Fourier transformed in the xy-plane the Green's dyadics in Eqs. (14) and (15) are defined in the Fourier space. For example, the electric Green's dyadic is defined as

$$\boldsymbol{\Gamma}(\mathbf{r}, \mathbf{r}'; \omega) = \int \frac{d^2 k_\perp}{(2\pi)^2} \, e^{i\mathbf{k}_\perp \cdot (\mathbf{r} - \mathbf{r}')_\perp} \boldsymbol{\gamma}(z, z'; \mathbf{k}_\perp, \omega). \tag{16}$$

The solutions to Eqs. (12) for the magnetic and electric Green's functions completely determine the fields by Eqs. (13). In other words, the boundary conditions for the fields on a semitransparent δ-function plate thus impose conditions on the magnetic and electric Green's functions at the position of the plate.

III.   MAGNETIC AND ELECTRIC GREEN'S FUNCTIONS

In this section we find solutions to the magnetic and electric Green's functions introduced in Eqs. (12) and satisfying boundary conditions dictated by Eqs. (10) and (11). Since we do not restrict our discussion to $\lambda_{e,g}^{||} = 0$, our solutions in this section could be used to analyze the alternative choices $E_3(a) = 0$ or $H_3(a) = 0$ in Eqs. (10a) and (11a). The treatment in this section considers a δ-function plate sandwiched between two uniaxial materials, described by

$$\boldsymbol{\varepsilon}(z) = \varepsilon^\perp(z) \, \mathbf{1}_\perp + \varepsilon^{||}(z) \, \hat{\mathbf{z}} \hat{\mathbf{z}}, \tag{17a}$$

$$\boldsymbol{\mu}(z) = \mu^\perp(z) \, \mathbf{1}_\perp + \mu^{||}(z) \, \hat{\mathbf{z}} \hat{\mathbf{z}}, \tag{17b}$$

where

$$\varepsilon^{\perp,||}(z) = 1 + (\varepsilon_1^{\perp,||} - 1)\theta(a - z) + (\varepsilon_2^{\perp,||} - 1)\theta(z - a) + \lambda_e^{\perp,||}\delta(z - a), \tag{18a}$$

$$\mu^{\perp,||}(z) = 1 + (\mu_1^{\perp,||} - 1)\theta(a - z) + (\mu_2^{\perp,||} - 1)\theta(z - a) + \lambda_g^{\perp,||}\delta(z - a). \tag{18b}$$
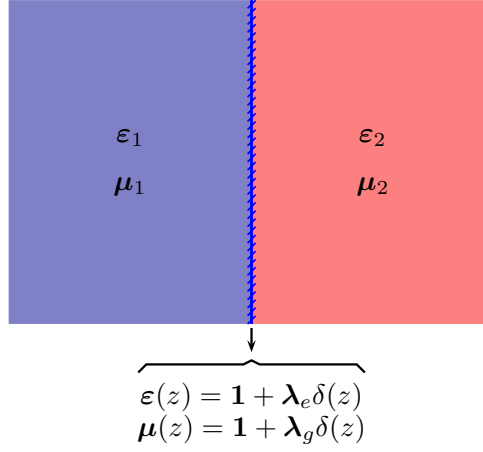
FIG. 1. A semitransparent δ-function plate sandwiched between two semi-infinite slabs with the material properties of Eq. (17).

We have used Heaviside step functions, or θ-functions,

$$\theta(z) = \begin{cases} 1 & \text{if} \quad z > 0, \\ 0 & \text{if} \quad z < 0, \end{cases} \tag{19}$$

and δ-functions in Eqs. (18) to describe discontinuities and singularities in the material properties. See Fig. 1. Setting $\varepsilon_i^\perp = \varepsilon_i^{||} = 1$ and $\mu_i^\perp = \mu_i^{||} = 1$ corresponds to a semitransparent δ-function plate in vacuum.

The boundary conditions on the fields of Eqs. (10) and (11) are transcribed onto the Green's dyadics through Eqs. (13). The boundary conditions on the TM mode in Eqs. (10) give the conditions

$$\varepsilon_2^{||} \gamma_{3i}(a+\delta, z') - \varepsilon_1^{||} \gamma_{3i}(a-\delta, z') = -ik_\perp \lambda_e^\perp \frac{1}{2} \big[\gamma_{1i}(a+\delta, z') + \gamma_{1i}(a-\delta, z') \big], \tag{20a}$$

$$\gamma_{1i}(a+\delta, z') - \gamma_{1i}(a-\delta, z') = i\omega \lambda_g^\perp \frac{1}{2} \big[\phi_{2i}(a+\delta, z') + \phi_{2i}(a-\delta, z') \big], \tag{20b}$$

and the corresponding boundary conditions on the TE mode in Eqs. (11) gives

$$\mu_2^{||} \phi_{3i}(a+\delta, z') - \mu_1^{||} \phi_{3i}(a-\delta, z') = -ik_\perp \lambda_g^\perp \frac{1}{2} \big[\phi_{1i}(a+\delta, z') + \phi_{1i}(a-\delta, z') \big], \tag{21a}$$

$$\phi_{1i}(a+\delta, z') - \phi_{1i}(a-\delta, z') = -i\omega \lambda_e^\perp \frac{1}{2} \big[\gamma_{2i}(a+\delta, z') + \gamma_{2i}(a-\delta, z') \big]. \tag{21b}$$

Using Eqs. (14) and (15), the boundary conditions in Eqs. (20) and (21) on the Green's dyadics in turn dictate the boundary conditions on the electric and magnetic Green's functions. These are more efficiently found by setting $i = 3$ in Eqs. (20) to obtain the boundary conditions on the magnetic Green's function,

$$g^H(z, z') \Big|_{z=a-\delta}^{z=a+\delta} = \frac{\lambda_e^\perp}{2} \left[\left\{ \frac{1}{\varepsilon^\perp(z)} \frac{\partial}{\partial z} g^H(z, z') \right\}_{z=a+\delta} + \left\{ \frac{1}{\varepsilon^\perp(z)} \frac{\partial}{\partial z} g^H(z, z') \right\}_{z=a-\delta} \right], \tag{22a}$$

$$\left\{ \frac{1}{\varepsilon^\perp(z)} \frac{\partial}{\partial z} g^H(z, z') \right\} \Big|_{z=a-\delta}^{z=a+\delta} = \zeta^2 \frac{\lambda_g^\perp}{2} \big[g^H(a+\delta, z') + g^H(a-\delta, z') \big]. \tag{22b}$$

Similarly, setting $i = 2$ in Eqs. (21) yields the boundary conditions on the electric Green's function,

$$g^E(z, z') \Big|_{z=a-\delta}^{z=a+\delta} = \frac{\lambda_g^\perp}{2} \left[\left\{ \frac{1}{\mu^\perp(z)} \frac{\partial}{\partial z} g^E(z, z') \right\}_{z=a+\delta} + \left\{ \frac{1}{\mu^\perp(z)} \frac{\partial}{\partial z} g^E(z, z') \right\}_{z=a-\delta} \right], \tag{23a}$$

$$\left\{ \frac{1}{\mu^\perp(z)} \frac{\partial}{\partial z} g^E(z, z') \right\} \Big|_{z=a-\delta}^{z=a+\delta} = \zeta^2 \frac{\lambda_e^\perp}{2} \big[g^E(a+\delta, z') + g^E(a-\delta, z') \big]. \tag{23b}$$

Note that we have switched to imaginary frequencies by performing the Euclidean rotation, $\omega \to i\zeta$.

The solution for the magnetic Green's function satisfying the boundary conditions in Eqs. (22) is

$$
g^H(z, z') = \begin{cases}
\frac{1}{2\bar{\kappa}_1^H}\left[e^{-\kappa_1^H|z-z'|} + r_{12}^H\, e^{-\kappa_1^H|z-a|}e^{-\kappa_1^H|z'-a|}\right], & \text{if} \quad z, z' < a, \\[8pt]
\frac{1}{2\bar{\kappa}_2^H}\left[e^{-\kappa_2^H|z-z'|} + r_{21}^H\, e^{-\kappa_2^H|z-a|}e^{-\kappa_2^H|z'-a|}\right], & \text{if} \quad a < z, z', \\[8pt]
\frac{1}{2\bar{\kappa}_2^H}\, t_{21}^H\, e^{-\kappa_1^H|z-a|}e^{-\kappa_2^H|z'-a|}, & \text{if} \quad z < a < z', \\[8pt]
\frac{1}{2\bar{\kappa}_1^H}\, t_{12}^H\, e^{-\kappa_2^H|z-a|}e^{-\kappa_1^H|z'-a|}, & \text{if} \quad z' < a < z,
\end{cases}
\tag{24}
$$

where the reflection coefficients are

$$
r_{ij}^H = \frac{\bar{\kappa}_i^H\left(1 + \frac{\lambda_e^\perp \bar{\kappa}_j^H}{2}\right)\left(1 - \frac{\lambda_g^\perp \zeta^2}{2\bar{\kappa}_i^H}\right) - \bar{\kappa}_j^H\left(1 - \frac{\lambda_e^\perp \bar{\kappa}_i^H}{2}\right)\left(1 + \frac{\lambda_g^\perp \zeta^2}{2\bar{\kappa}_j^H}\right)}{\bar{\kappa}_i^H\left(1 + \frac{\lambda_e^\perp \bar{\kappa}_j^H}{2}\right)\left(1 + \frac{\lambda_g^\perp \zeta^2}{2\bar{\kappa}_i^H}\right) + \bar{\kappa}_j^H\left(1 + \frac{\lambda_e^\perp \bar{\kappa}_i^H}{2}\right)\left(1 + \frac{\lambda_g^\perp \zeta^2}{2\bar{\kappa}_j^H}\right)},
\tag{25}
$$

and the transmission coefficients are

$$
t_{ij}^H = \frac{\bar{\kappa}_i^H\left(1 + \frac{\lambda_e^\perp \bar{\kappa}_i^H}{2}\right)\left(1 - \frac{\lambda_g^\perp \zeta^2}{2\bar{\kappa}_i^H}\right) + \bar{\kappa}_i^H\left(1 - \frac{\lambda_e^\perp \bar{\kappa}_i^H}{2}\right)\left(1 + \frac{\lambda_g^\perp \zeta^2}{2\bar{\kappa}_i^H}\right)}{\bar{\kappa}_i^H\left(1 + \frac{\lambda_e^\perp \bar{\kappa}_j^H}{2}\right)\left(1 + \frac{\lambda_g^\perp \zeta^2}{2\bar{\kappa}_i^H}\right) + \bar{\kappa}_j^H\left(1 + \frac{\lambda_e^\perp \bar{\kappa}_i^H}{2}\right)\left(1 + \frac{\lambda_g^\perp \zeta^2}{2\bar{\kappa}_j^H}\right)},
\tag{26}
$$

with

$$
\kappa_i^H = \sqrt{k_\perp^2 \frac{\varepsilon_i^\perp}{\varepsilon_i^{||}} + \zeta^2 \varepsilon_i^\perp \mu_i^\perp} \qquad \text{and} \qquad \bar{\kappa}_i^H = \frac{\kappa_i^H}{\varepsilon_i^\perp} = \sqrt{\frac{k_\perp^2}{\varepsilon_i^\perp \varepsilon_i^{||}} + \zeta^2 \frac{\mu_i^\perp}{\varepsilon_i^\perp}}.
\tag{27}
$$

The electric Green's function is obtained from the magnetic Green's function by replacing $\boldsymbol{\varepsilon} \leftrightarrow \boldsymbol{\mu}$ and $H \to E$, with the corresponding definitions

$$
\kappa_i^E = \sqrt{k_\perp^2 \frac{\mu_i^\perp}{\mu_i^{||}} + \zeta^2 \mu_i^\perp \varepsilon_i^\perp} \qquad \text{and} \qquad \bar{\kappa}_i^E = \frac{\kappa_i^E}{\mu_i^\perp} = \sqrt{\frac{k_\perp^2}{\mu_i^\perp \mu_i^{||}} + \zeta^2 \frac{\varepsilon_i^\perp}{\mu_i^\perp}}.
\tag{28}
$$

Setting $\lambda_e^\perp = \lambda_g^\perp = 0$, Eqs. (25) and (26) immediately leads to the standard reflection and transmission coefficients at the interface of two semi-infinite slabs, and serves as a check for the reflection and transmission coefficients in Eqs. (25) and (26).

It should be emphasized that even though we explicitly considered materials with $\lambda_e^{||}$ and $\lambda_g^{||}$ in Eqs. (18), the solutions to the Green's functions given by Eqs. (24) through (28) are independent of $\lambda_e^{||}$ and $\lambda_g^{||}$. The Green's functions of Eqs. (24) determine the fields unambiguously everywhere (except on the δ-function plate) and the implication is that there are no observable consequences of $\lambda_e^{||}$ and $\lambda_g^{||}$.

A. Green's functions for a semitransparent δ-function plate

A semitransparent δ-function plate in vacuum corresponds to setting $\varepsilon_i^\perp = \varepsilon_i^{||} = 1$ and $\mu_i^\perp = \mu_i^{||} = 1$. This simplifies the expressions for the reflection and transmission coefficients in Eqs. (25) and (26) significantly because κ_i^H and κ_i^E no longer are distinct. In terms of

$$
\kappa^2 = k_\perp^2 + \zeta^2,
\tag{29}
$$

the magnetic Green's function for a semitransparent δ-function plate in vacuum can be expressed in the compact form

$$
g^H(z, z') = \frac{1}{2\kappa}e^{-\kappa|z-z'|} + \left[r_g^H + \eta(z-a)\eta(z'-a)\, r_e^H\right]\frac{1}{2\kappa}e^{-\kappa|z-a|}e^{-\kappa|z'-a|},
\tag{30}
$$

where

$$
\eta(z) = \begin{cases} 1, & \text{if} \quad z > 0, \\ -1, & \text{if} \quad z < 0. \end{cases}
\tag{31}
$$

Equation (30) is written in terms of contributions to the reflection coefficients of the transverse magnetic mode for the two special cases of vanishing electric permittivity and vanishing magnetic permeability. These reflection coefficients, r_e^H and r_g^H, and the corresponding transmission coefficients, t_e^H and t_g^H, are related by,

$$r_e^H = \frac{\lambda_e^\perp}{\lambda_e^\perp + \frac{2}{\kappa}}, \quad t_e^H = 1 - r_e^H, \qquad \text{and} \qquad r_g^H = -\frac{\lambda_g^\perp}{\lambda_g^\perp + \frac{2\kappa}{\zeta^2}}, \quad t_g^H = 1 + r_g^H. \tag{32}$$

The total reflection and transmission coefficients for the magnetic mode (easily read off from Eq. (30) with reference to Eqs. (24)) are

$$r^H = r_g^H + r_e^H, \qquad t^H = 1 + r_g^H - r_e^H. \tag{33}$$

In terms of these reflection coefficients the boundary conditions for the magnetic Green's function in Eqs. (22) read

$$\left[1 + r^H - t^H\right] = \frac{\lambda_e^\perp \kappa}{2}\left[1 - r^H + t^H\right], \tag{34a}$$

$$\left[1 - r^H - t^H\right] = \frac{\lambda_g^\perp \zeta^2}{2\kappa}\left[1 + r^H + t^H\right]. \tag{34b}$$

Combining Eqs. (34) is expected to yield the statement of conservation of energy for the TM-mode [27],

$$1 - (r^H)^2 - (t^H)^2 = \frac{1}{2}\frac{\lambda_e^\perp \kappa}{2}\left[1 - r^H + t^H\right]^2 + \frac{1}{2}\frac{\lambda_g^\perp \zeta^2}{2\kappa}\left[1 + r^H + t^H\right]^2. \tag{35}$$

This calls for an investigation of conservation of energy in the presence of a semitransparent δ-function plate. From Maxwell's equations in Eqs. (3) the local statement of conservation of energy is,

$$\boldsymbol{\nabla} \cdot (\mathbf{E} \times \mathbf{H}) + \mathbf{E} \cdot \frac{\partial}{\partial t}\mathbf{D} + \mathbf{H} \cdot \frac{\partial}{\partial t}\mathbf{B} = 0. \tag{36}$$

It equates the energy flux into a volume with the rate of change of the energy density. When integrated across the δ-function plate in the $\hat{\mathbf{z}}$-direction this yields Eq. (35) and thus verifies that our description by a δ-function plate conserves energy. It is to be noted that the terms on the left hand side in Eq. (35) come from the energy flux term in Eq. (36), and the terms on the right hand side are contributed by the energy density.

From the general solution in Eq (30) one can read off the contributions for the special case when the δ-function plate is purely electric ($r_g^H = 0$), or when the δ-function plate is purely magnetic ($r_e^H = 0$). A perfect electrical conductor is a material with $r_e^H = 1$ and $r_g^H = 0$. This is found by taking the limit $\lambda_e^\perp \to \infty$ and $\lambda_g^\perp = 0$ in Eq. (32). Similarly, a perfect magnetic conductor, described by $r_e^H = 0$ and $r_g^H = -1$, is obtained when $\lambda_e^\perp = 0$ and $\lambda_g^\perp \to \infty$. A perfect electric and magnetic conductor interestingly is described by $r_e^H = 1$ and $r_g^H = -1$. This corresponds to $r^H = 0$ and $t^H = -1$, and implies the total transmission of an incident wave with a phase shift of π when crossing the δ-function plate. Insertion of such a plate in a circular laser would extinguish it if the circumference equals an integer multiple of the wavelength of the laser.

Similar expressions hold for the electric Green's function obtained by swapping $\lambda_e^\perp \leftrightarrow \lambda_g^\perp$ and replacing superscripts $H \to E$.

B. Boundary conditions on a perfect electrically conducting δ-function plate

Before we consider a perfect electrically conducting δ-function plate, let us first consider the boundary conditions at the interface of two semi-infinite dielectric slabs with $\varepsilon_1 \ll \varepsilon_2$, with no δ-function plate sandwiched in between, $\boldsymbol{\lambda}_e = \boldsymbol{\lambda}_g = 0$. Boundary conditions on the TM-mode in Eqs. (10) for this case read $\varepsilon_2^{||} E_3(a + \delta) = \varepsilon_1^{||} E_3(a - \delta)$, and $E_1(a + \delta) = E_1(a - \delta)$, with no information content in Eqs. (10a). Using the solutions for the Green's functions in Eq. (24) we can evaluate the electric fields using Eqs. (13). For convenience let us choose the polarization source to be a polarized point source $\mathbf{P} \propto (1, 0, 0)\,\delta^{(3)}(\mathbf{x} - \mathbf{x}')$ outside the interface. With the intention of taking the limit of infinite dielectric response in the slab on the right, $\varepsilon_2 \to \infty$, we choose the source point just to the left, $z' = a - \delta$, because it is meaningless to have an electromagnetic source inside a perfect conductor. In this manner we can show that: $E_1(a + \delta) = E_1(a - \delta) = -\bar{\kappa}_1^H(1 - r_{12}^H)/2$, and $\varepsilon_2^{||} E_3(a + \delta) = \varepsilon_1^{||} E_3(a - \delta) = -ik_\perp(1 + r_{12}^H)/2$. For the case when the second medium is perfectly conducting in the xy-plane, we have $\varepsilon_2^\perp \to \infty$ and $r_{12}^H \to 1$, which implies:

$E_1(a+\delta) = E_1(a-\delta) = 0$, and $\varepsilon_2^{||} E_3(a+\delta) = \varepsilon_1^{||} E_3(a-\delta) = -ik_\perp$. Thus perfect conduction in xy-plane alone sets the tangential component of electric field to zero, but does not require the normal component of electric field to be zero. If we further require infinite conductance in the z-direction, we have $\varepsilon_2^{||} \to \infty$, which implies: $E_3(a-\delta) = -ik_\perp/\varepsilon_1^{||}$ and $E_3(a+\delta) = 0$. These are the boundary conditions satisfied by the electric field on a perfect isotropic conductor. Notice the interesting fact that with normal component of electric field being zero inside the conductor and with infinite dielectric response in the z-direction inside the conductor, we still have a well defined finite value for the normal component of the electric displacement field, $\lim_{\varepsilon_2^\perp \to \infty, \varepsilon_2^{||} \to \infty} D_3(a+\delta) = -ik_\perp$. This is necessary to satisfy the continuity condition for the normal component of the macroscopic field at the interface.

Let us next consider a semitransparent electric δ-function plate in vacuum by setting $\boldsymbol{\varepsilon}_1 = \boldsymbol{\varepsilon}_2 = 1$ and $\boldsymbol{\lambda}_g = 0$. In principle now there is no need to restrict the source point to $z' = a - \delta$. For this case we can evaluate

$$E_1(a) = E_1(a+\delta) = E_1(a-\delta) = -\frac{\kappa}{2}(1 - r_e^H) \xrightarrow{\lambda_e^\perp \to \infty} 0, \tag{37}$$

where we used the limiting condition, $r_e^H \to 1$, using Eq. (32). Similarly, we can evaluate, for $z' = a - \delta$,

$$E_3(a+\delta) = -\frac{ik_\perp}{2}(1 - r_e^H) \xrightarrow{\lambda_e^\perp \to \infty} 0, \tag{38a}$$

$$E_3(a-\delta) = -\frac{ik_\perp}{2}(1 + r_e^H) \xrightarrow{\lambda_e^\perp \to \infty} -ik_\perp. \tag{38b}$$

When the source is placed at an arbitrary distance z' all the above expressions contain an exponentially decaying factor of $\exp(-\kappa|z' - a|)$. We further note that the factor contributing on the right hand side of Eq. (10b) is

$$\lambda_e^\perp E_1(a) = -r_e^H \xrightarrow{\lambda_e^\perp \to \infty} -1. \tag{39}$$

Thus, there is no distinction between a semi-infinite perfect isotropic electric conductor and a perfect electrically conducting δ-function plate. To clarify how these two cases conspire to yield the same physics in the perfect conducting limit we rewrite Eq. (10b) in the form

$$D_3(a-\delta) = D_3(a+\delta) + ik_\perp \lambda_e^\perp E_1(a) = \begin{cases} -ik_\perp + 0, & \text{for} \quad \boldsymbol{\lambda}_e = \mathbf{0}, \quad \boldsymbol{\varepsilon}_2 = \varepsilon_2 \mathbf{1} \to \infty, \\ 0 - ik_\perp, & \text{for} \quad \lambda_e^\perp \to \infty, \quad \boldsymbol{\varepsilon}_2 = \mathbf{1}, \end{cases} \tag{40}$$

where we explicitly note that while for a semi-infinite perfect isotropic electric conductor the contribution on the right is from $D_3(a+\delta)$, for a perfect electrically conducting δ-function plate the contribution is from the term contributing on the δ-function plate.

Similar analysis for the TE-mode leads to the corresponding boundary conditions on the magnetic fields.

IV. PHYSICAL REALIZATION OF A SEMITRANSPARENT δ-FUNCTION PLATE

From this point on, to simplify the analysis, we consider a purely electrical material by considering the special case $\lambda_g^\perp = 0$. Further, we shall emphasize the frequency dependence by writing $\lambda_e^\perp(i\zeta)$.

In Refs. [11, 12] Barton considers an infinitesimally thin plasma sheet carrying a continuous fluid with surface charge and current densities modelled in terms of the fluid displacement which is assumed to be purely tangential. Barton's hydrodynamical model is identical to our consideration here if we require the frequency response to be

$$\lambda_e^\perp(i\zeta) = \frac{\zeta_p}{\zeta^2}, \tag{41}$$

where the parameter ζ_p corresponds to the characteristic wavenumber in Barton's model [11].

A. Thin-plate limit

We begin by inquiring, in what approximation will a dielectric slab of thickness d simulate a (purely electric) semitransparent δ-function plate? To this end we write the δ-function in Eq. (1a) in terms of θ-functions,

$$\varepsilon^{\perp,||}(i\zeta) - 1 = \lambda_e^{\perp,||}(i\zeta) \lim_{d\to 0} \frac{[\theta(z+d) - \theta(z)]}{d}, \tag{42}$$

which in the limit $d \to 0$ exactly yields Eq. (1a). Equation (42) describes a dielectric slab of thickness d if we read the factor $\lambda_e^{\perp,||}(i\zeta)/d$ to represent the slab's susceptibility.

One can find the reflection coefficients for the TM–and TE-modes for the dielectric slab described by Eq. (42) after solving the corresponding Green's functions in Eqs. (12), see for example Ref. [22]. We show that when the following conditions for the thin-plate limit are met,

$$\zeta^2 \ll \frac{\zeta_p}{d} \ll \frac{1}{d^2}, \qquad \text{and} \qquad k_\perp^2 \ll \frac{\zeta_p}{d} \ll \frac{1}{d^2}, \tag{43}$$

the reflection coefficients for the TM–and TE-modes for a dielectric slab of thickness d have the following limiting behavior [22],

$$r_{\text{thick}}^H = -\left(\frac{\bar{\kappa}_i^H - \kappa}{\bar{\kappa}_i^H + \kappa}\right) \frac{(1 - e^{-2\kappa_i^H d})}{\left[1 - \left(\frac{\bar{\kappa}_i^H - \kappa}{\bar{\kappa}_i^H + \kappa}\right)^2 e^{-2\kappa_i^H d}\right]} \xrightarrow[\substack{k_\perp d \ll \sqrt{\zeta_p d} \ll 1}]{\zeta d \ll \sqrt{\zeta_p d} \ll 1} r_e^H = \frac{\lambda_e^\perp(i\zeta)}{\lambda_e^\perp(i\zeta) + \frac{2}{\kappa}}, \tag{44a}$$

$$r_{\text{thick}}^E = -\left(\frac{\kappa_i^E - \kappa}{\kappa_i^E + \kappa}\right) \frac{(1 - e^{-2\kappa_i^E d})}{\left[1 - \left(\frac{\kappa_i^E - \kappa}{\kappa_i^E + \kappa}\right)^2 e^{-2\kappa_i^E d}\right]} \xrightarrow[\substack{k_\perp d \ll \sqrt{\zeta_p d} \ll 1}]{\zeta d \ll \sqrt{\zeta_p d} \ll 1} r_e^E = -\frac{\lambda_e^\perp(i\zeta)}{\lambda_e^\perp(i\zeta) + \frac{2\kappa}{\zeta^2}}, \tag{44b}$$

where r_e^H and r_e^E are the corresponding reflection coefficients in Eq.(32) for a purely electric δ-function plate. The variables κ_i^H and κ_i^E in Eqs. (44) are given by setting $\mu^\perp = \mu^{||} = 1$ in Eqs. (27) and (28). The above limiting behavior is derived in the following manner. Using Eq. (42) we have the dielectric permittivity of the slab given by $(\varepsilon^\perp - 1) = 1/x$ in terms of $x = d/\lambda_e^\perp$. We then consider the approximations

$$-\frac{\bar{\kappa}_i^H - \kappa}{\bar{\kappa}_i^H + \kappa} = 1 - 2c\sqrt{x} + \mathcal{O}(x^{3/2}), \tag{45a}$$

$$e^{-2\kappa_i^H d} = 1 - 2\kappa c\sqrt{x}\frac{\zeta_p}{\zeta^2} + \mathcal{O}(x^{3/2}, \zeta\sqrt{\lambda_e^\perp d}), \tag{45b}$$

which then implies the limiting behavior in Eq. (44a). Similarly one derives Eq. (44b). The factor $c = \bar{\kappa}_i^H \sqrt{\varepsilon^\perp}/\kappa$ in Eqs. (45) cancels out in the limiting behavior. The approximations $x \ll 1$ and $\zeta^2 \lambda_e^\perp d \ll 1$ necessary for the approximations in Eqs. (45) to be valid are the approximations for the thin-plate limit which was presented in Eq. (43) in a compact form. Thus, we have shown that the reflection coefficients of a dielectric slab reduce to those of a δ-function plate in the thin-plate limit of Eq. (43). The limiting behavior in Eqs. (44) is a straightforward generalization of the analysis for the isotropic case carried out in Ref. [22], and should be contrasted with setting $d = 0$ in r_{thick}^H and r_{thick}^E, which would imply zero reflectance and suggest non-existence of the plate in this limit. Note that the reflection coefficients for the thick slab on the left hand side of Eqs. (44) contains $\varepsilon^{||}$ inside the variables κ_i^H and κ_i^E, but the limiting behavior on the right hand side of Eqs. (44) is completely unaware of any dependence on $\varepsilon^{||}$. Thus, in the thin-plate limit of Eq. (43) the optical properties only depend on the transverse properties of the plate.

B. Plasma sheet

Combining Eq. (41), with the dielectric model in Eq. (42) for the case of a plasma model, we can identify the plasma frequency, $\omega_p^2 = n_f e^2/m = \zeta_p/d$, for the thin plasma sheet, where n_f is the number density of charge carriers with charge e and mass m. The implication seems to be that the number density is inversely proportional to the thickness of the material for a very thin plasma sheet. To analyze this we model the charge carriers as a non-relativistic Fermi gas, confined in a slab of thickness d that is infinite in extent along the xy-directions, with energy states

$$E_n(\mathbf{k}_\perp) = \frac{1}{2m}\left[\mathbf{k}_\perp^2 + n^2\frac{\pi^2}{d^2}\right], \qquad n = 0, 1, 2, \dots, \tag{46}$$

where n represents the discretization due to confinement in the z-direction. Notice that $n = 0$ state is not excluded because one imposes the Neumann boundary condition, which is necessary to have no probability flux across the walls of the slab. The total number of charge carriers, n_{tot}, in the slab is obtained by summing over all the occupied energy states. Thus, in terms of the Fermi energy, $E_F = k_F^2/2m$, one evaluates the number density,

$$n_f = \frac{n_{\text{tot}}}{A\,d} = 2\frac{1}{d}\sum_{n=0}^{\infty}\int_{-\infty}^{\infty}\frac{dk_x}{2\pi}\int_{-\infty}^{\infty}\frac{dk_y}{2\pi}\,\theta(E_F - E_n(k_x, k_y)) = \frac{k_F^3}{3\pi^2}\nu(x), \tag{47}$$
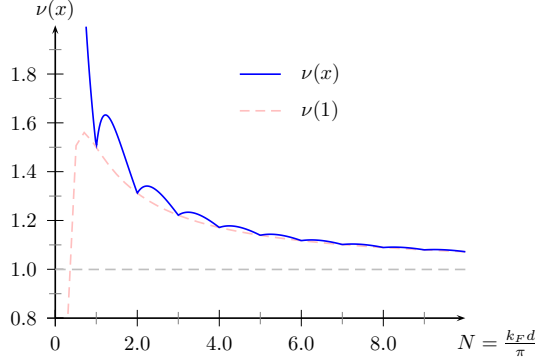
FIG. 2. Plot of $\nu(x)$ in Eq. (48) versus $N = k_F d/\pi$. The value of $\nu(1)$ and of $N \to \infty$ limit are also shown.

where A is the area of the plate, and the factor 2 in the second equality is introduced to accommodate two Fermi charges in each energy state. The thickness dependence of the number density is captured in the function

$$\nu(x) = \frac{3}{2}\left(x - \frac{1}{3}x^3\right) + \frac{3}{2N}\left(1 - \frac{1}{2}x^2\right) - \frac{1}{4N^2}x, \tag{48}$$

where $x = [N]/N$ is the fractional floor function, $[N]$ referring to the integer part of $N = k_F d/\pi$. For a sufficiently thick slab the difference between $[N]$ and N is negligible, thus $x \to 1$ and $\nu(x) \to 1$. A thin plate corresponds to small values of N, and in particular for $N < 1$ we have $\nu(x) \to 3/2N$. The function $\nu(x)$ has been plotted in Fig. 2. The limiting cases of the function $\nu(x)$ determine the number density in Eq. (47) for these situations [9, 28],

$$n_f = \frac{n_{\text{tot}}}{A\,d} \to \begin{cases} \frac{k_F^2}{2\pi d} & \text{if} \quad N < 1 \quad \text{(2-D sheet)}, \\ \frac{k_F^3}{3\pi^2} & \text{if} \quad N \to \infty \quad \text{(3-D bulk)}. \end{cases} \tag{49}$$

It is suggestive to explore the physical nature of the condition $N < 1$, which states $d^2 n_{\text{tot}}/A < \pi/2$. Introducing the packing fraction of a material defined as $\nu_0 = N_{\text{atoms}} A_{\text{atom}}/A$, in terms of the total number of atoms N_{atoms}, and area of an atom $A_{\text{atom}} = \pi a_0^2$ with a_0 being the radius of the atom, we recognize that the condition $N < 1$ corresponds to the window $1 \leq d/2a_0 < \pi/\sqrt{8\nu_0 n_0} \sim 1$, where the inequality on the left is imposed because a thin sheet of material has to be at least one layer of atom thick. The total number of carrier charges per atom is defined to be n_0. The packing fraction is always less than unity, $\nu_0 < 1$. Thus, the condition $N < 1$ states that a one-atom-layer thick material behaves like a two-dimensional sheet unless the packing fraction is very low.

Using the number density for a two-dimensional sheet from Eq. (49) in conjunction with Eq. (41) and $\omega_p^2 = n_f e^2/m$ we identify

$$\zeta_p = \frac{e^2}{m} \frac{n_{\text{tot}}}{A}. \tag{50}$$

In this manner ζ_p is interpreted as a plasma frequency of a two-dimensional plasma sheet [9, 11].

V. CASIMIR INTERACTION ENERGY BETWEEN TWO SEMITRANSPARENT δ-FUNCTION PLATES

In this section we calculate the Casimir interaction energy between two parallel semitransparent δ-function plates located at $z = a_1$ and $z = a_2$, with $a = a_2 - a_1 > 0$. The Casimir interaction energy between two disjoint planar objects may be calculated using the multiple scattering formalism

$$\frac{E_{12}}{A} = \frac{1}{2} \int_{-\infty}^{\infty} \frac{d\zeta}{2\pi} \int \frac{d^2 k_\perp}{(2\pi)^2} \text{Tr} \ln\left[\mathbf{1} - \boldsymbol{\gamma}_1 \cdot \mathbf{V}_1 \cdot \boldsymbol{\gamma}_2 \cdot \mathbf{V}_2\right], \tag{51}$$

where the objects in Eq. (51) are described by the potentials representing the dielectric response functions, $\mathbf{V}_i(z) = \varepsilon_i(z) - \mathbf{1}$, which for δ-function plates are described by Eqs. (1a) and (2a) with $\lambda_{ei}^{||} = 0$, with subscripts $i = 1, 2$,

standing for the respective plates. See Fig. 3(a). The trace, Tr, in Eq. (51) is over both the space coordinate and dyadic index. For the case under consideration the trace on the coordinate index can be moved inside the logarithm. Further, the δ-functions in the potentials from Eq. (1a) allow the integrals in the trace over the space coordinate to be performed and yields

$$\frac{E_{12}^{\delta\text{-plate}}}{A} = \frac{1}{2}\int_{-\infty}^{\infty}\frac{d\zeta}{2\pi}\int\frac{d^2k_\perp}{(2\pi)^2}\,\text{tr}\ln\left[\mathbf{1} - \boldsymbol{\gamma}_1(a_2,a_1)\cdot\boldsymbol{\lambda}_1\cdot\boldsymbol{\gamma}_2(a_1,a_2)\cdot\boldsymbol{\lambda}_2\right], \tag{52}$$

in which the trace, tr, is only on the dyadic index. We point out that semitransparent δ-function plates being considered are necessarily anisotropic and $\boldsymbol{\lambda}_{ei} = \lambda_{ei}^\perp(i\zeta)\,\text{diag}(1,1,0)$. Evaluation of $\boldsymbol{\gamma}_1(a_2,a_1)$ and $\boldsymbol{\gamma}_2(a_1,a_2)$, see Appendix B for details, lets us express Eq. (52) in the form

$$\frac{E_{12}^{\delta\text{-plate}}}{A} = \frac{1}{2}\int_{-\infty}^{\infty}\frac{d\zeta}{2\pi}\int\frac{d^2k_\perp}{(2\pi)^2}\left\{\ln\left[1 - r_{e1}^H r_{e2}^H\,e^{-2\kappa a}\right] + \ln\left[1 - r_{e1}^E r_{e2}^E\,e^{-2\kappa a}\right]\right\}, \tag{53}$$

in terms of the reflection coefficients for the separate modes due to a semitransparent δ-function plate in Eq. (32). Equation (53) could have immediately been written down once the reflection coefficients were known, because using multiple reflections the Casimir energy is determined by the reflection coefficients geometrically.

For a perfect electrically conducting δ-function plate we take the limit ($\lambda_{ei}^\perp \to \infty$), for which we have $r_{ei}^H \to 1$, $r_{ei}^E \to -1$. Using this in Eq. (53) we have the interaction energy between two perfect electrically conducting δ-function plates,

$$\frac{E_{12}^{\text{Cas}}}{A} = \frac{1}{2}\int_{-\infty}^{\infty}\frac{d\zeta}{2\pi}\int\frac{d^2k}{(2\pi)^2}\,2\ln\left[1 - e^{-2\kappa a}\right] = -\frac{\pi^2}{720\,a^3}, \tag{54}$$

which is exactly the Casimir energy between two perfect electrically conducting plates [2]. This conclusion is in agreement with the result in Ref. [17].

A. Thin-plate limit of Casimir interaction energy for two anisotropic slabs

In Sec. IV we showed that the reflection coefficient of a thick dielectric slab reduces to that of a semitransparent δ-function plate in the thin-plate limit of Eq. (43). Since the Casimir energy involves integrating over all frequencies it is of interest to see how the conditions in Eq. (43) translate for the case of Casimir energies. Specifically, we ask under what conditions does the Casimir interaction energy of two anisotropic slabs reduce to that of two semitransparent δ-function plates? To this end we follow the derivation of Lifshitz energy between two anisotropic slabs in the spirit of Ref. [22], with details provided in Appendix C.

The interaction energy between two anisotropic slabs is given by Eq. (51) when the slabs are described by the potentials

$$\mathbf{V}_i(z) = (\boldsymbol{\varepsilon}_i - \mathbf{1})\big[\theta(z - a_i) - \theta(z - b_i)\big], \qquad i = 1, 2, \tag{55}$$

where $b_i - a_i = d_i$ are the thicknesses of the slabs, and $a_2 - b_1 = a$ is the distance between the slabs. See Fig. 3(b). We shall consider an anisotropic dielectric tensor of the form $\boldsymbol{\varepsilon}_i = \text{diag}(\varepsilon_i^\perp, \varepsilon_i^\perp, \varepsilon_i^{||})$. The interaction energy of two such slabs is given by Eq. (53) with the following replacements in the reflection coefficients: $r_{ei}^H \to r_{\text{thick}}^{H,i}$, and $r_{ei}^E \to r_{\text{thick}}^{E,i}$, see Appendix C for details,

$$\frac{E_{12}^{\text{thick}}}{A} = \frac{1}{2}\int_{-\infty}^{\infty}\frac{d\zeta}{2\pi}\int\frac{d^2k}{(2\pi)^2}\left\{\ln\left[1 - r_{\text{thick}}^{H,1} r_{\text{thick}}^{H,2}\,e^{-2\kappa a}\right] + \ln\left[1 - r_{\text{thick}}^{E,1} r_{\text{thick}}^{E,2}\,e^{-2\kappa a}\right]\right\}, \tag{56}$$

which again could have immediately been written down once the reflection coefficients were obtained.

We have earlier shown that when the conditions for the thin-plate limit in Eq. (43) are met the reflection coefficients of a thick anisotropic slab transforms into the corresponding reflection coefficients for a δ-function plate, see Eqs. (44). Since the thin-plate limit of Eq. (43) puts bounds on frequencies and wavenumbers, the thin-plate limit of the Casimir energy between two anisotropic slabs is estimated by introducing cutoffs in the integrals of Eq. (56),

$$\frac{E_{12,\text{TP-limit}}^{\text{thick}}}{A} = \frac{1}{2}\int_{-\sqrt{\frac{\varsigma_p}{d}}}^{\sqrt{\frac{\varsigma_p}{d}}}\frac{d\zeta}{2\pi}\int_{-\sqrt{\frac{\varsigma_p}{d}}}^{\sqrt{\frac{\varsigma_p}{d}}}\frac{d^2k}{(2\pi)^2}\left\{\quad\cdots\quad\right\}, \tag{57}$$

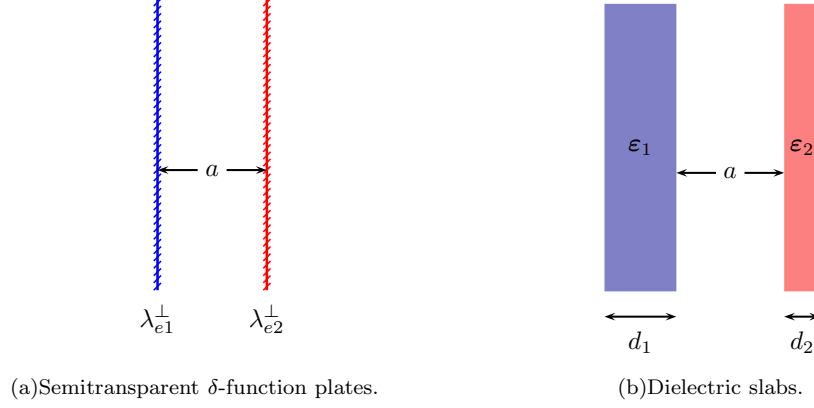(a)Semitransparent δ-function plates.

(b)Dielectric slabs.

FIG. 3. (a) Parallel semitransparent δ-function plates separated by distance a. (b) Parallel anisotropic dielectric slabs of thicknesses d_i separated by distance a.
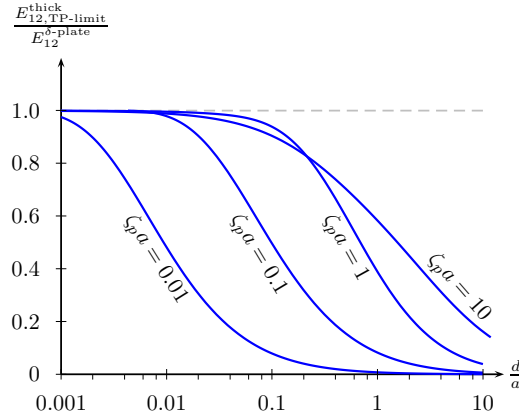

FIG. 4. Plotted on the ordinate is the ratio of the thin-plate limit of the interaction energy of two anisotropic dielectric slabs in Eq. (57) to the interaction energy of two δ-function plates in Eq. (53). The fractional error is plotted with respect to d/a on a logarithmic scale for different values of $\zeta_p a$. The ratio is minimized in the thin-plate limit, $d/a \ll \zeta_p a \ll a/d$.

where the reflection coefficients inside the curly brackets are obtained using the thin-plate limit of Eq. (43) as in Eqs. (44). After scaling the integral variables with the distance between the plates we observe that Eq. (57) is a good approximation of the interaction energy between two δ-plates of Eq. (53) in the parameter regime

$$\frac{d}{a} \ll \zeta_p a \ll \frac{1}{d/a}, \tag{58}$$

which is obtained by rearranging Eq. (43) after recognizing that typical values of frequencies contributing to the integral are of the order $\zeta \sim 1/a$. This has been illustrated in Fig. 4 where we plot the ratio of this thin-plate limit of the interaction energy of two anisotropic dielectric slabs in Eq. (57) to the interaction energy of two δ-function plates in Eq. (53).

VI. CASIMIR-POLDER INTERACTION ENERGY BETWEEN AN ATOM AND A δ-FUNCTION PLATE

In this section we calculate the Casimir-Polder interaction energy between an atom and a semitransparent δ-function plate. We demonstrate that the same result is obtained in the thin-plate limit of Eq. (58) for the Casimir-Polder interaction energy between an atom and a dielectric slab. For a perfect electrically conducting δ-function plate we show

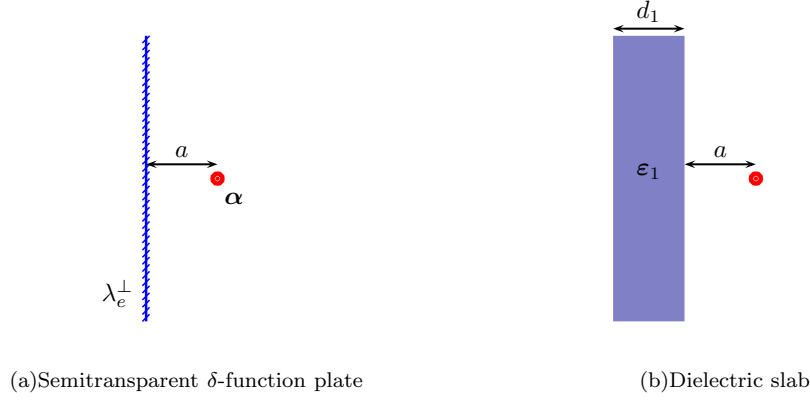(a)Semitransparent δ-function plate

(b)Dielectric slab

FIG. 5. Anisotropic atom in front of (a) a semitransparent δ-function plate, versus (b) an anisotropic dielectric slab.

that this energy is exactly equal to the corresponding energy between an atom and a perfect electrically conducting plate.

A.   Atom in front of a δ-function plate

We consider an atom with anisotropic electric dipole polarizability $\boldsymbol{\alpha} = \text{diag}(\alpha^\perp, \alpha^\perp, \alpha^{||})$ in front of a semitransparent δ-function plate described by Eqs. (1a) and (2a) with $\lambda_{ei}^{||} = 0$. The potential for an atom when one neglects quadruple and higher moments is $\mathbf{V}(\mathbf{x}) = 4\pi\,\boldsymbol{\alpha}(i\zeta)\,\delta^{(3)}(\mathbf{x} - \mathbf{x}_0)$, where $\mathbf{x}_0$ is the position of the atom and $\boldsymbol{\alpha}(i\zeta)$ is the atomic dipole polarizability of the atom. An atom in this model is described by at least two parameters, one corresponding to the static polarizability $|\boldsymbol{\alpha}(0)|$, and the other corresponding to the resonant frequency ω_i of the atom. The weak approximation of the interaction energy in Eq. (51), valid for separation distances $r \gg |\boldsymbol{\alpha}(0)|^{1/3}$, consists of retaining only the leading term of the logarithm after expansion. This approximation is valid for $|\boldsymbol{\alpha}(0)|^{1/3}$ small compared to separation distances. The unretarded (van der Waals-London) regime ($|\boldsymbol{\alpha}(0)|^{1/3} < r \ll c/\omega_i$) is a short-range approximation, and the retarded (Casimir-Polder) regime ($|\boldsymbol{\alpha}(0)|^{1/3} < c/\omega_i \ll r$) is the corresponding long-range approximation, where short and long is in relation to the characteristic length associated with resonant frequency. Note that both the van der Waals-London interaction energy and the Casimir-Polder interaction energy are intrinsically weak.

The expression for Casimir-Polder energy is obtained by retaining the leading term in the logarithm and replacing $\boldsymbol{\gamma}_2$ with the free Green's dyadic $\boldsymbol{\gamma}_0$ in Eq. (51), which for planar geometries is given by the formula

$$E_{12}^{\text{CP}} = -2\pi \int_{-\infty}^{\infty} \frac{d\zeta}{2\pi} \int \frac{d^2 k_\perp}{(2\pi)^2} \int_{-\infty}^{\infty} dz\, \text{tr}\Big[\boldsymbol{\alpha} \cdot \boldsymbol{\gamma}_1(a, z) \cdot \mathbf{V}_1(z) \cdot \boldsymbol{\gamma}_0(z - a)\Big], \tag{59}$$

where trace, tr, is over the dyadic index and a is the distance between the atom, and the δ-function plate is described by $\mathbf{V}_1(z) = \boldsymbol{\lambda}_e\,\delta(z)$, with $\boldsymbol{\lambda}_e = \lambda_e^\perp \,\text{diag}(1, 1, 0)$. Performing the z-integral yields

$$E_{12}^{\text{CP}} = -2\pi \int_{-\infty}^{\infty} \frac{d\zeta}{2\pi} \int \frac{d^2 k_\perp}{(2\pi)^2}\, \text{tr}\Big[\boldsymbol{\alpha} \cdot \boldsymbol{\gamma}_1(a, 0) \cdot \boldsymbol{\lambda}_e \cdot \boldsymbol{\gamma}_0(-a)\Big]. \tag{60}$$

Using Eqs. (B1) to evaluate $\boldsymbol{\gamma}_1(a, 0)$, and using the expression for the free Green's dyadic in the form

$$\boldsymbol{\gamma}_0(z) = \begin{bmatrix} -\kappa^2 & 0 & -ik_\perp \kappa \eta(z) \\ 0 & -\zeta^2 & 0 \\ -ik_\perp \kappa \eta(z) & 0 & k_\perp^2 \end{bmatrix} \frac{1}{2\kappa}\, e^{-\kappa|z|}, \tag{61}$$

with $\eta(z)$ defined in Eq. (31), into Eq. (60), one calculates the Casimir-Polder energy between an atom and a δ-function plate to be

$$E_{12}^{\text{CP}} = -2\pi \int_{-\infty}^{\infty} \frac{d\zeta}{2\pi} \int \frac{d^2 k_\perp}{(2\pi)^2}\, \frac{e^{-2\kappa a}}{2\kappa} \Big[\alpha^\perp (\kappa^2 r_e^H - \zeta^2 r_e^E) + \alpha^{||} k_\perp^2\, r_e^H\Big]. \tag{62}$$

The above expression for atoms with isotropic polarizabilities interacting with plates having finite thickness was probably first reported in Ref. [29]. In the long distance limit the Casimir-Polder energy gets contributions from the polarizabilities for very low frequencies. Thus, we replace the atomic polarizabilities in Eq. (62) by the static polarizabilities $\boldsymbol{\alpha}(0)$ though the reflection coefficients are ζ dependent. The Casimir-Polder energy between an atom and a perfect electrically conducting δ-function plate is obtained from Eq. (62) by setting $r_e^H = 1$ and $r_e^E = -1$, in which case the integrals in Eq. (62) can be completed to yield

$$E_{12}^{\mathrm{CP}} = -\frac{\mathrm{tr}(\boldsymbol{\alpha})}{8\pi a^4}, \tag{63}$$

which is exactly the Casimir-Polder energy between an atom and a perfect electrically conducting plate.

B. Thin-plate limit of Casimir-Polder energy for an atom in front of an anisotropic dielectric slab

Let us next consider an atom in front of an anisotropic dielectric slab of thickness d described by the potential $\mathbf{V}_1(z) = (\boldsymbol{\varepsilon} - 1)[\theta(z + d) - \theta(z)]$, with $\boldsymbol{\varepsilon} = \mathrm{diag}(\varepsilon^\perp, \varepsilon^\perp, \varepsilon^{||})$. See Fig. 5(b). Using this in Eq. (59) the Casimir-Polder energy for an atom in front of a dielectric slab is given by

$$E_{12}^{\mathrm{CP}} = -2\pi \int_{-\infty}^{\infty} \frac{d\zeta}{2\pi} \int \frac{d^2 k_\perp}{(2\pi)^2} \int_{-d}^{0} dz\, \mathrm{tr}\Big[\boldsymbol{\alpha} \cdot \boldsymbol{\gamma}_1(a, z) \cdot (\boldsymbol{\varepsilon} - 1) \cdot \boldsymbol{\gamma}_0(z - a)\Big]. \tag{64}$$

Using Eq. (C4) to evaluate $\boldsymbol{\gamma}_1(a, z) \cdot (\boldsymbol{\varepsilon} - 1)$, and using Eq. (61) to evaluate the free Green's dyadic, in Eq. (64) we obtain the Casimir-Polder energy for an atom in front of an anisotropic dielectric slab expressed in the form of Eq. (62) with the replacements: $r_e^{H,E} \to r_{\mathrm{thick}}^{H,E}$, in terms of the reflection coefficients of the anisotropic slab. Using the limiting behavior of the reflection coefficients in Eq. (44) valid when the conditions in Eq. (43) are met we then immediately obtain the thin-plate limit to match the expression in Eq. (62) for the Casimir-Polder energy for an atom interacting with a δ-function plate. As noted earlier this introduces a cutoff on the integrals and thus is valid in the regime of the thin-plate limit given by Eq. (58).

C. Bordag's "thick" and "thin" boundary conditions

Bordag [17] claims there are two types of perfect electrically conducting boundary conditions. In both cases the tangential components of the electric field must vanish on the surface S,

$$\mathbf{n} \times \mathbf{E}\Big|_S = 0, \tag{65}$$

where $\mathbf{n}$ is the normal vector to the surface. However, he states that for a "thick" conductor, there is an additional condition on the normal component of the electric field at the surface:

$$\frac{\partial}{\partial n} E_n\Big|_S = 0, \tag{66}$$

while for a "thin" conductor there is no further constraint on E_n. This distinction is difficult to understand, because Maxwell's equations should have essentially unique solutions given the boundary condition (65) on a closed surface [30]. How indeed is it possible to impose an additional condition on the electric field? In fact, Gauss' law in the form ($\varepsilon = 1$, Heaviside-Lorentz units)

$$\boldsymbol{\nabla} \cdot \mathbf{E} = \rho, \tag{67}$$

in terms of the charge density ρ, says, very close to a conducting surface S

$$\frac{\partial}{\partial n} E_n(\mathbf{r})\Big|_{\mathbf{r} \to S} = \delta(\mathbf{r} \cdot \mathbf{n})\sigma(\mathbf{r}_\perp), \tag{68}$$

which implies the usual statement

$$E_n\Big|_S = \sigma \tag{69}$$

on the surface, in terms of the surface charge density σ. The latter for a conductor is not a specifiable quantity, but must be determined by solving for the electric field configuration. The *limit* of the condition (68) as the surface is approached is, in fact, just Eq. (65).

Bordag computes photon propagators in terms of vector potentials in both of these scenarios. He shows that if these propagators are used to compute Casimir forces between conducting bodies, the same results emerge independent of which propagator is used. However, when applied to the Casimir-Polder interaction between a polarizable atom and a conducting plate, the two propagators give different results. The "thick" propagator gives the conventional result in Eq. (63). Using the "thin" propagator, he obtains, for isotropic polarizability, a result which is smaller by a factor of 13/15, which is within the measurement uncertainty of the experiment [31].

On the other hand, the Casimir-Polder force can be computed from the electric Green's dyadic [26]:

$$\mathbf{\Gamma}(\mathbf{r}, t; \mathbf{r}', t') = i\langle \mathbf{E}(\mathbf{r}, t)\mathbf{E}(\mathbf{r}', t')\rangle, \tag{70}$$

which is a gauge-invariant quantity. In terms of the frequency Fourier transform of this, we can write the Casimir-Polder energy as

$$U_{\mathrm{CP}} = \frac{i}{2}\int \frac{d\omega}{2\pi}4\pi\mathrm{tr}\,\boldsymbol{\alpha}(\omega)\mathbf{\Gamma}(\mathbf{R}, \mathbf{R}, \omega), \tag{71}$$

where $\mathbf{R}$ denotes the position of the atom. In Ref. [26] the isotropic version of Eq. (63) is obtained, with no ambiguity in electromagnetic boundary conditions. However, in the Appendix of that paper, a propagator in terms of the potentials was also defined:

$$A_\mu(x) = \int d^4x' D_{\mu\nu}(x, x')J^\nu(x') + \partial_\mu\lambda, \tag{72}$$

where J^ν is the (conserved) electric current density, and λ is arbitrary gauge function. Maxwell's equations read

$$L^{\mu\nu}A_\nu = J^\mu, \tag{73}$$

where the differential operator is in vacuum ($\varepsilon = \mu = 1$)

$$L^{\mu\nu} = \partial^\mu\partial^\nu - g^{\mu\nu}\partial^2, \quad \partial^2 = \nabla^2 - \partial_0^2. \tag{74}$$

The corresponding propagator must satisfy

$$L^{\mu\alpha}L'^{\nu\beta}D_{\alpha\beta} = L^{\mu\nu}\delta(x - x'). \tag{75}$$

Reference [17] presents two propagators, satisfying the thick and thin boundary conditions, on a conducting surface at $z = 0$. We will write these in the form

$$D_{\mu\nu}(x, x') = D_{\mu\nu}^{(0)}(x - x') + \bar{D}_{\mu\nu}(x, x'), \tag{76}$$

where the free propagator has the expected form

$$D_{\mu\nu}^{(0)}(x - x') = g_{\mu\nu}\int \frac{d\omega}{2\pi}\frac{(d^3\mathbf{k})}{(2\pi)^3}e^{-i\omega(t-t')}e^{i\mathbf{k}\cdot(\mathbf{r}-\mathbf{r}')}\frac{1}{k^2}, \tag{77}$$

in the metric $g_{\mu\nu} = \mathrm{diag}(-1, 1, 1, 1)$, $k^2 = -(k^0)^2 + \mathbf{k}^2$, $k^0 = \omega$. We have further noted that any tensor structure in the propagator proportional to ∂_μ or ∂'_ν will vanish when acted upon by $L^{\mu\alpha}$, $L'^{\nu\beta}$. It is easy to confirm that $D_{\mu\nu}^{(0)}$ satisfies Eq. (75). So $\bar{D}_{\mu\nu}$ must satisfy the corresponding homogeneous equation.

Let us first check this for the conventional "thick" propagator, which Bordag writes in the form

$$\bar{D}_{\mu\nu}(x, x') = \int \frac{d\omega}{2\pi}\frac{(d^2\mathbf{k}_\perp)}{(2\pi)^2}\frac{dk_3}{2\pi}e^{-i\omega(t-t')}e^{i\mathbf{k}_\perp\cdot(\mathbf{r}-\mathbf{r}')_\perp}e^{ik_3(|z|+|z'|)}\frac{\bar{g}_{\mu\nu}}{k^2}, \tag{78}$$

where

$$\bar{g}_{\mu\nu} = \mathrm{diag}(-1, 1, 1, -1). \tag{79}$$

This is constructed so that the D_{33} component vanishes on the plane $z = 0$. Now a straightforward calculation shows that

$$L^{\mu\alpha}L'^{\nu\beta}\bar{D}_{\alpha\beta} = \int \frac{d\omega}{2\pi}\frac{(d^2\mathbf{k}_\perp)}{(2\pi)^2}\frac{dk_3}{2\pi}e^{-i\omega(t-t')}e^{i\mathbf{k}_\perp\cdot(\mathbf{r}-\mathbf{r}')_\perp}e^{ik_3(|z|+|z'|)}M^{\mu\nu}(k), \tag{80}$$

where

$$M^{\mu\nu}(k) = \begin{pmatrix} -\mathbf{k}^2 & -k^0 k_1 & -k^0 k_2 & k^0 k_3 \\ -k^0 k_1 & k_1^2 + k_3^2 - (k^0)^2 & -k_1 k_2 & k_1 k_3 \\ -k^0 k_2 & -k_1 k_2 & k_1^2 + k_3^2 - (k^0)^2 & k_2 k_3 \\ -k^0 k_3 & -k_1 k_3 & -k_2 k_3 & (k^0)^2 - \mathbf{k}_\perp^2 \end{pmatrix}. \tag{81}$$

Notice that the k^2 in the denominator has cancelled out, and that therefore k_3 only occurs in the numerator, and consequently when the integral over k_3 is carried out, we obtain either $\delta(|z|+|z'|)$ or derivatives thereof. Since $|z|+|z'|$ is never zero unless both points lie on the surface, we obtain the required zero value.

The "thin" propagator is given by Bordag in terms of specific polarization vectors. We content ourselves with writing the appropriate metric tensor in Eq. (78), which follows from those, in terms of $\kappa^2 = \mathbf{k}_\perp^2 - (k^0)^2$:

$$\bar{g}_{\mu\nu} = \sum_{s=1,2} E_\mu^s E_\nu^s = -\frac{1}{\kappa^2} \begin{pmatrix} \mathbf{k}_\perp^2 & -k^0 k_1 & -k^0 k_2 & 0 \\ -k^0 k_1 & (k^0)^2 - k_2^2 & k_1 k_2 & 0 \\ -k^0 k_2 & k_1 k_2 & (k^0)^2 - k_1^2 & 0 \\ 0 & 0 & 0 & 0 \end{pmatrix}, \tag{82}$$

where E_μ^s is defined in Ref. [17]. Then inserting this into the Maxwell equation we obtain a result in the form of Eq. (80) with the tensor

$$\frac{1}{k^2} M^{\mu\nu}(k) = -\frac{1}{\kappa^2} \begin{pmatrix} \mathbf{k}_\perp^2 & k^0 k_1 & k^0 k_2 & 0 \\ k^0 k_1 & (k^0)^2 - k_2^2 & k_1 k_2 & 0 \\ k^0 k_2 & k_1 k_2 & (k^0)^2 - k_1^2 & 0 \\ 0 & 0 & 0 & 0 \end{pmatrix}, \tag{83}$$

which differs simply by some signs from Eq. (82). Again, this may be argued to be zero because k_3 only occurs in the numerator, so the integration over k_3 vanishes.

So the two potential propagators satisfy the same Maxwell equation, and satisfy, we believe, the same physical boundary conditions, so they should be gauge-equivalent. We verify this by showing that they both correspond to the same electric Green's dyadic, that given in Ref. [26]. In that reference, because we are dealing with a cylindrically symmetric (isotropic) geometry, without loss of generality we took $\mathbf{k}_\perp = (k_1, 0)$. Then from the usual construction of the field strength tensor,

$$F^{\mu\nu} = \partial^\mu A^\nu - \partial^\nu A^\mu, \tag{84}$$

from which $\mathbf{E}_i = F^{0i}$, and the electric Green's dyadic of Eq. (70) can be immediately obtained from the propagators given above. In fact, using either propagator we find

$$\mathbf{\Gamma}(\mathbf{r}, t; \mathbf{r}', t') = \mathbf{\Gamma}^{(0)}(\mathbf{r} - \mathbf{r}', t - t') + \bar{\mathbf{\Gamma}}(\mathbf{r}, t; \mathbf{r}', t') \tag{85}$$

where

$$\bar{\mathbf{\Gamma}}(\mathbf{r}, t; \mathbf{r}', t') = \int \frac{d\omega}{2\pi} \frac{(d^2 \mathbf{k}_\perp)}{(2\pi)^2} e^{-i\omega(t-t')} e^{i\mathbf{k}_\perp \cdot (\mathbf{r}-\mathbf{r}')_\perp} \bar{\boldsymbol{\gamma}}(z, z'), \tag{86}$$

with

$$\bar{\boldsymbol{\gamma}}(z, z') = \begin{pmatrix} -\kappa^2 & 0 & i\kappa k_\perp \\ 0 & \omega^2 & 0 \\ -i\kappa k_\perp & 0 & -k_\perp^2 \end{pmatrix} \frac{1}{2\kappa} e^{-\kappa(|z|+|z'|)}, \tag{87}$$

which is exactly the Green's dyadic given in Ref. [26]. So the two propagators correspond to precisely the same physical situation, and are just expressed in different gauges. The apparently singular $1/\kappa^2$ term (singular in Minkowski space) in Eq. (83) has no untoward consequences, but is necessary to establish this coincidence. Therefore, we conclude that the usual Casimir-Polder force between a conducting plate and a polarizable atom is correct, irrespective of whether the plate is "thick" or "thin."

VII. CONCLUSION AND OUTLOOK

We have considered an infinitesimally thin material whose optical properties are given in terms of a δ-function. By integrating across the plate we have derived the boundary conditions on such a δ-function plate in Eqs. (10) and (11). The Green's dyadic for a δ-function plate, which completely determines its optical properties, has been derived. The optical properties of a δ-function plate are shown to necessarily be anisotropic in that they only depend on the transverse properties of the plate. Our work generalizes Barton's insightful work on the subject in Refs. [11, 12] for magnetic materials. We have shown that Bordag's "thick" and "thin" boundary conditions on a perfect conductor are identical to Barton's boundary conditions, which resolves the controversy on the uniqueness of the boundary conditions for a perfect conductor.

To understand the physical content of our results for a δ-function plate we defined the thin-plate limit, given by Eq. (43) for reflection coefficients and by Eq. (58) for Casimir energies, and clarified how a δ-function plate is physically realized as an infinitesimally thin plate. We have shown that in the thin-plate limit of Eq. (43) the reflection coefficients of a dielectric slab reduce to those of a δ-function plate. The thin-plate limit of the interaction energy between two anisotropic slabs is shown to be the Casimir energy between two δ-function plates. Similarly, the thin-plate limit of the interaction energy between an atom and an anisotropic slab is shown to be the Casimir-Polder energy between an atom and a δ-function plate.

The reflection coefficients obtained for a δ-function plate in Eq. (32) are very general because they are independent of the dispersion model used to represent $\lambda_e^\perp(i\zeta)$ and $\lambda_g^\perp(i\zeta)$. In our discussions, from Sec. IV onwards, we exclusively used the plasma model for a 2-dimensional metal to represent $\lambda_e^\perp(i\zeta)$. Since the thin-plate limit of Eq. (43) is a constraint on the frequency response, the definition of thin-plate limit will depend on the dispersion model used to represent $\lambda_e^\perp(i\zeta)$. Thus, the thin-plate limit defined in Eq. (43) is specific for a plasma model and is sufficient as long as the relevant frequencies are large compared to relaxation frequency. The corresponding thin-plate limit when the low frequency limit of the Drude model represents $\lambda_e^\perp(i\zeta)$ is being employed by us to model graphene, which we believe will lead to interesting insights into the quantum electromagnetic interactions of graphene.

ACKNOWLEDGMENTS

Appendix A: Proof for "averaging prescription"

Let us consider a function $f(x)$ with a step discontinuity

$$f(x) = a_1\,\theta(-x) + a_2\,\theta(x), \tag{A1}$$

written using the θ-function of Eq. (19), whose value at $x = 0$, $f(0)$, is not well defined. If we now evaluate the integral, using the standard prescription, we obtain

$$\int_{-\infty}^{\infty} dx\,\delta(x)f(x) = f(0), \tag{A2}$$

which in turn now is not well defined.

The δ-function can be interpreted as a limit of a sequence of functions

$$\delta(x) = \lim_{\epsilon \to 0} u_\epsilon(x), \tag{A3}$$

each of which satisfies

$$\int_{-\infty}^{\infty} dx\,u_\epsilon(x) = 1. \tag{A4}$$

For our purpose, we shall restrict to functions that are symmetric with respect to the origin [21]

$$u_\epsilon(-x) = u_\epsilon(x). \tag{A5}$$

Using the representation of the δ-function in Eq. (A3) to evaluate the integral in Eq. (A2) we obtain

$$\int_{-\infty}^{\infty} dx\, \delta(x) f(x) = a_1 \lim_{\epsilon \to 0} \int_{-\infty}^{0} dx\, u_\epsilon(x) + a_2 \lim_{\epsilon \to 0} \int_{0}^{\infty} dx\, u_\epsilon(x) \tag{A6a}$$

$$= \left(\frac{a_1 + a_2}{2} \right) \int_{-\infty}^{\infty} dx\, u_\epsilon(x) \tag{A6b}$$

$$= \frac{a_1 + a_2}{2}, \tag{A6c}$$

where we used the symmetry restriction of Eq. (A5) in the second equality. Using the result in Eq. (A6c) to define the value of $f(0)$ in Eq. (A2) we have

$$f(0) = \frac{a_1 + a_2}{2}, \tag{A7}$$

which is the averaging prescription.

We shall point to Ref. [21] for discussions and references on this topic.

Appendix B: Evaluation of Green's dyadics for a δ-function plate

Evaluation of $\gamma_1(a_2, a_1)$ in Eq. (51) is performed using Eq. (14) in terms of the magnetic Green's function in Eq. (30) with $r_g^H = 0$ and the dielectric functions of the media appearing in Eq. (14) being set to unity because we are considering δ-function plates in vacuum. The corresponding electric Green's function is obtained by interchanging the electric and magnetic properties. Furthermore, these Green's functions are evaluated on the position of the plates using the averaging prescription [24]. In the evaluation of $\gamma_1(a_2, a_1)$ we use

$$g_1^E(z, z')\big|_{z=a_2, z'=a_1} = \frac{1}{\zeta^2} \frac{1}{\left[\lambda_{e1}^\perp(i\zeta) + \frac{2\kappa}{\zeta^2} \right]} e^{-\kappa a}, \tag{B1a}$$

$$\partial_{z'} g_1^H(z, z')\big|_{z=a_2, z'=a_1} = \frac{1}{\kappa} \frac{1}{\left[\lambda_{e1}^\perp(i\zeta) + \frac{2}{\kappa} \right]} e^{-\kappa a}, \tag{B1b}$$

$$\partial_z \partial_{z'} g_1^H(z, z')\big|_{z=a_2, z'=a_1} = -\frac{1}{\left[\lambda_{e1}^\perp(i\zeta) + \frac{2}{\kappa} \right]} e^{-\kappa a}, \tag{B1c}$$

which using Eq. (14) yields $\gamma_1(a_2, a_1)$.

Appendix C: Lifshitz interaction energy for anisotropic dielectric slabs

For the case of two anisotropic slabs (with isotropy in the plane of the slabs) the Green's dyadic in Eq. (14) can be decomposed into magnetic and electric modes, and we can can write the Casimir energy per unit area in the form

$$\frac{E_{12}^{\text{thick}}}{L_x L_y} = \frac{1}{2} \int_{-\infty}^{\infty} \frac{d\zeta}{2\pi} \int \frac{d^2 k_\perp}{(2\pi)^2} \left\{ \ln\left[1 - K^E\right] + \ln\left[1 - K^H\right] \right\}, \tag{C1}$$

where

$$K^E = (\varepsilon_1^\perp - 1)(\varepsilon_2^\perp - 1)\zeta^4 \int_{a_1}^{b_1} dz \int_{a_2}^{b_2} dz'\, g_1^E(z', z) g_2^E(z, z'), \tag{C2}$$

$$K^H = \int_{a_1}^{b_1} dz \int_{a_2}^{b_2} dz'\, \text{tr}\left[\boldsymbol{\gamma}_1^H(z', z) \cdot (\boldsymbol{\varepsilon}_1 - \mathbf{1}) \cdot \boldsymbol{\gamma}_2^H(z, z') \cdot (\boldsymbol{\varepsilon}_2 - \mathbf{1}) \right]. \tag{C3}$$

The regions for evaluation of z and z' are unambiguously specified by the integration regions. Notice that we can omit the δ-function term in Eq. (14) since z and z' are never evaluated at the same point for disjoint objects. Thus we can write

$$\boldsymbol{\gamma}_1^H(z',z) \cdot (\boldsymbol{\varepsilon}_1 - \mathbf{1}) = \left[\begin{array}{cc} \partial_z \partial_{z'} g_1^H(z',z) & ik_\perp \partial_{z'} g_1^H(z',z) \\ -ik_\perp \partial_z g_1^H(z',z) & k_\perp^2 g_1^H(z',z) \end{array} \right] \left[\begin{array}{cc} (\varepsilon_1^\perp - 1)/\varepsilon_1^\perp & 0 \\ 0 & (\varepsilon_1^{||} - 1)/\varepsilon_1^{||} \end{array} \right], \tag{C4}$$

where we have used the fact that the Green's function for the first slab, $g_1^H(z',z)$, evaluated for $a_1 < z < b_1$ and $a_2 < z' < b_2$ corresponds to choosing $\boldsymbol{\varepsilon}_1(z) = \boldsymbol{\varepsilon}_1$, and $\boldsymbol{\varepsilon}_1(z') = \mathbf{1}$. Similarly,

$$\boldsymbol{\gamma}_2^H(z,z') \cdot (\boldsymbol{\varepsilon}_2 - \mathbf{1}) = \left[\begin{array}{cc} \partial_z \partial_{z'} g_2^H(z,z') & ik_\perp \partial_z g_2^H(z,z') \\ -ik_\perp \partial_{z'} g_2^H(z,z') & k_\perp^2 g_1^H(z,z') \end{array} \right] \left[\begin{array}{cc} (\varepsilon_2^\perp - 1)/\varepsilon_2^\perp & 0 \\ 0 & (\varepsilon_2^{||} - 1)/\varepsilon_2^{||} \end{array} \right], \tag{C5}$$

observing that the Green's function for the second slab, $g_2^H(z,z')$, evaluated for $a_1 < z < b_1$ and $a_2 < z' < b_2$ corresponds to choosing $\boldsymbol{\varepsilon}_2(z) = \mathbf{1}$, and $\boldsymbol{\varepsilon}_2(z') = \boldsymbol{\varepsilon}_2$.

The magnetic Green's functions for $a_1 < z < b_1$ and $a_2 < z' < b_2$ for the respective slabs are [22]

$$g_1^H(z',z) = \frac{e^{-\kappa(z'-b_1)} \left[(\bar{\kappa}_1^H + \kappa) e^{-\kappa_1^H(b_1-z)} + (\bar{\kappa}_1^H - \kappa) e^{-\kappa_1^H d_1} e^{-\kappa_1^H(z-a_1)} \right]}{\left[(\bar{\kappa}_1^H + \kappa)^2 - (\bar{\kappa}_1^H - \kappa)^2 e^{-2\kappa_1^H d_1} \right]}, \tag{C6a}$$

$$g_2^H(z,z') = \frac{e^{-\kappa(a_2-z)} \left[(\bar{\kappa}_2^H + \kappa) e^{-\kappa_2^H(z'-a_2)} + (\bar{\kappa}_2^H - \kappa) e^{-\kappa_2^H d_2} e^{-\kappa_2^H(b_2-z')} \right]}{\left[(\bar{\kappa}_2^H + \kappa)^2 - (\bar{\kappa}_2^H - \kappa)^2 e^{-2\kappa_2^H d_2} \right]}, \tag{C6b}$$

and the corresponding electric Green's function is obtained by swapping the electric and magnetic properties. We have used the definitions for κ_i^H's and κ_i^E's in Eqs. (27) and (28) with $\boldsymbol{\mu} = \mathbf{1}$. Completing the algebra we have the interaction energy between parallel anisotropic slabs presented in Eq. (56) and written in terms of the reflection coefficients for a thick anisotropic slab introduced in Eqs. (44).

[1] T. H. Boyer, "Quantum electromagnetic zero point energy of a conducting spherical shell and the Casimir model for a charged particle," Phys. Rev. **174**, 1764 (1968).
[2] H. B. G. Casimir, "On the attraction between two perfectly conducting plates," Kon. Ned. Akad. Wetensch. Proc. **51**, 793 (1948).
[3] C. M. Bender and K. A. Milton, "Casimir effect for a D-dimensional sphere," Phys. Rev. D **50**, 6547 (1994), arXiv:hep-th/9406048 [hep-th].
[4] E. K. Abalo, K. A. Milton, and L. Kaplan, "Casimir energies of cylinders: Universal function," Phys. Rev. D **82**, 125007 (2010), arXiv:1008.4778 [hep-th].
[5] E. K. Abalo, K. A. Milton, and L. Kaplan, "Scalar Casimir energies of tetrahedra and prisms," (2012), arXiv:1202.0908 [hep-th].
[6] G. Barton, "Casimir energies of spherical plasma shells," J. Phys. A: Math. Gen. **37**, 1011 (2004).
[7] G. Barton, "Casimir's spheres near the Coulomb limit: Energy density, pressures and radiative effects," J. Phys. A: Math. Gen. **37**, 3725 (2004).
[8] G. Barton, "Casimir's spheres near the Coulomb limit: Energy density, pressures and radiative effects," J. Phys. A: Math. Gen. **37**, 11945 (2004).
[9] A. L. Fetter, "Electrodynamics of a layered electron gas. I. Single layer," Annals of Physics **81**, 367 (1973).
[10] A. L. Fetter, "Electrodynamics of a layered electron gas. II. Periodic array," Annals of Physics **88**, 1 (1974).
[11] G. Barton, "Casimir effects for a flat plasma sheet: I. Energies," J. Phys. A: Math. Gen. **38**, 2997 (2005).
[12] G. Barton, "Casimir effects for a flat plasma sheet: II. Fields and stresses," J. Phys. A: Math. Gen. **38**, 3021 (2005).
[13] M. Bordag, D. Robaschik, and E. Wieczorek, "Quantum field theoretic treatment of the Casimir effect," Annals of Physics **165**, 192 (1985).
[14] M. Bordag, D. Hennig, and D. Robaschik, "Vacuum energy in quantum field theory with external potentials concentrated on planes," J. Phys. A: Math. Gen. **25**, 4483 (1992).
[15] D. Robaschik and E. Wieczorek, "Pressure fluctuations and the quantization of electrodynamics with boundary conditions," Annals of Physics **236**, 43 (1994).
[16] M. Bordag, "The Casimir effect for thin plasma sheets and the role of the surface plasmons," J. Phys. A: Math. Gen. **39**, 6173 (2006).
[17] M. Bordag, "Reconsidering the quantization of electrodynamics with boundary conditions and some measurable consequences," Phys. Rev. D **70**, 085010 (2004).
[18] M. Bordag, "Interaction of a charge with a thin plasma sheet," Phys. Rev. D **76**, 065011 (2007).

[19] M. Scandurra, "The ground state energy of a massive scalar field in the background of a semi-transparent spherical shell," J. Phys. A: Math. Gen. **32**, 5679 (1999).

[20] M. Bordag and D. V. Vassilevic, "Heat kernel expansion for semitransparent boundaries," J. Phys. A: Math. Gen. **32**, 8247 (1999).

[21] R. Estrada and S. A. Fulling, "Functions and distributions in spaces with thick points," J. Appl. Math. Stat. **10**, 25 (2007).

[22] P. Parashar, *Geometrical investigations of the Casimir effect: Thickness and corrugations dependencies*, Ph.D. thesis, The University of Oklahoma, Norman (2011).

[23] C. D. Fosco, F. C. Lombardo, and F. D. Mazzitelli, "Derivative expansion of the electromagnetic Casimir energy for two thin mirrors," Phys. Rev. D **85**, 125037 (Jun 2012).

[24] I. Cavero-Pelaez, K. A. Milton, P. Parashar, and K. V. Shajesh, "Non-contact gears. I. Next-to-leading order contribution to lateral Casimir force between corrugated parallel plates," Phys. Rev. D **78**, 065018 (2008), arXiv:0805.2776 [hep-th].

[25] I. Cavero-Pelaez, K. A. Milton, P. Parashar, and K. V. Shajesh, "Non-contact gears. II. Casimir torque between concentric corrugated cylinders for the scalar case," Phys. Rev. D **78**, 065019 (2008), arXiv:0805.2777 [hep-th].

[26] J. Schwinger, L. L. DeRaad, Jr., and K. A. Milton, "Casimir effect in dielectrics," Annals Phys. **115**, 1 (1978).

[27] J. Schwinger, L. L. DeRaad, Jr., K. A. Milton, and Wu-yang Tsai, *Classical electrodynamics*, Advanced book program (Perseus Books, 1998).

[28] N. W. Ashcroft and N. D. Mermin, *Solid state physics* (Holt, Rinehart and Winston, New York, 1976).

[29] F. Zhou and L. Spruch, "van der Waals and retardation (Casimir) interactions of an electron or an atom with multilayered walls," Phys. Rev. A **52**, 297 (1995).

[30] K. A. Milton and J. Schwinger, *Electromagnetic Radiation: Variational Methods, Waveguides and Accelerators* (Springer-Verlag, Berlin, 2006).

[31] C. I. Sukenik, M. G. Boshier, D. Cho, V. Sandoghdar, and E. A. Hinds, "Measurement of the Casimir-Polder force," Phys. Rev. Lett. **70**, 560 (1993)
.